



CO₂
Human
Emissions

The CHE Tier2 Global Nature Run

Anna Agustí-Panareda

Joe McNorton

che-project.eu



Co-ordinated by
 ECMWF



CO₂ Human Emissions

D2.6 Global Run V2

Dissemination Level:	Public
Author(s):	Anna Agusti-Panareda, Joe McNorton, Margarita Choulga (ECMWF)
Date:	20/12/2019
Version:	1.0
Contractual Delivery Date:	31/12/2019
Work Package/ Task:	WP2/ T2.3
Document Owner:	ECMWF
Contributors:	ECMWF
Status:	Final



CO₂ Human Emissions

CHE: CO₂ Human Emissions Project

Coordination and Support Action (CSA)
H2020-EO-3-2017 Preparation for a European
capacity to monitor CO₂ anthropogenic emissions

Project Coordinator: Dr Gianpaolo Balsamo (ECMWF)
Project Start Date: 01/10/2017
Project Duration: 39 months

Published by the CHE Consortium

Contact:

ECMWF, Shinfield Park, Reading, RG2 9AX,
gianpaolo.balsamo@ecmwf.int



The CHE project has received funding from the European Union's Horizon 2020 research and innovation programme under grant agreement No 776186.



Table of Contents

1	Executive Summary	7
2	Introduction	7
2.1	Background.....	7
2.2	Scope of this deliverable	8
2.2.1	Objectives of this deliverable	8
2.2.2	Work performed in this deliverable	8
2.2.3	Deviations and counter measures.....	8
3	Model configuration.....	8
3.1	Experiment set up.....	9
3.2	Model output.....	10
4	Atmospheric tracer variability on seasonal, synoptic and diurnal scales.....	12
4.1	Plumes.....	14
4.2	Surface variability.....	15
4.3	Total column variability	18
4.4	Interpreting total column variability with tagged tracers	21
5	Ensemble simulations	22
5.1	Transport uncertainty estimates	23
5.2	Sensitivity to anthropogenic emissions.....	24
6	Potential applications	25
7	Conclusion	26
8	Acknowledgements.....	26
9	References	26
10	Annex: Prescribed emissions	31

Figures

- Figure 1 XCO₂ [ppm] spatial distribution on 1 January 2015 12 UTC. Values above and below the global mean in reds and greens respectively (see colour bar). 13
- Figure 2 XCO₂ [ppm] spatial distribution on 1 January 2015 12 UTC over Europe. Values above and below the global mean in reds and greens respectively (see colour bar). 13
- Figure 3 XCO₂ enhancement and depletion (see colour bar in ppm) associated with the total CO₂ flux at the surface (i.e. anthropogenic and biogenic) on 01 January 2015 after 12 hours of simulation in the CHE Tier2 9km nature run. Light blue colour show CO₂ depletion associated with natural sinks and yellow/red colours show enhancement associated with CO₂ sources..... 13
- Figure 4 XCO₂ enhancement and depletion (see colour bar in ppm) associated with (a) biogenic fluxes; (b) total anthropogenic emissions; (c) average power stations (excluding super power stations); (d) residential heating, (e) industry/manufacturing; and

- (f) transport (excluding aviation) on 02 January 2015 after 24 hours of simulation in the CHE Tier2 9km nature run..... 14
- Figure 5: Daily mean surface CO₂ at four NOAA baseline stations: brw (Barrow, Alaska, USA), mlo (Mauna Loa, Hawaii, USA at 71.3°N 156.6°W, 11 m a.s.l), smo (Tutuila, American Samoa, USA at 14.25°S 170.6°W, 42 m a.s.l), spo (South Pole, Antarctica at 89.9°S 24.8°W, 2810 m a.s.l) from the Tier 1 nature run (blue) , Tier 2 nature run (red), Tier 2 simulation at lower resolution (yellow) and observations (black). The observations have been obtained from the NOAA ObsPack (2017). The bias, standard error and root mean square error (rmse) are shown at the top of each panel, together with the sampling height [m] for each station. Note that Tier 2 stops in July because at the time of writing the deliverable the nature run experiment had not finished. The station sampling height is provided on the top left of each panel..... 16
- Figure 6 Daily mean surface CH₄ at three NOAA baseline stations: brw (Barrow, Alaska, USA), mlo (Mauna Loa, Hawaii, USA at 71.3°N 156.6°W, 11 m a.s.l), smo (Tutuila, American Samoa, USA at 14.25°S 170.6°W, 42 m a.s.l) from the Tier 1 nature run (blue), Tier 2 nature run (red), Tier 2 simulation at lower resolution (yellow) and observations (black). The observations have been obtained from the NOAA ObsPack (2017). The bias, standard error and root mean square error (rmse) are shown at the top of each panel, together with the sampling height [m] from each station. Note that Tier 2 stops in July because at the time of writing the deliverable the nature run experiment had not finished. The station sampling height is provided on the top left of each panel..... 16
- Figure 7: Hourly surface CO₂ at three in situ stations in North America: abt (Abbotsford, British Columbia, Canada at 49.03°N 122.37°W and 100m a.s.l, Environment Canada) from the Tier 1 nature run (T1_OA, blue), Tier 2 nature run (T2_EA, red) and observations (black) in July 2015. The observations have been obtained from the NOAA ObsPack (2017). The bias, standard error and root mean square error (rmse) are shown at the top of each panel, together with the sampling height [m] for each station. The station sampling height is provided on the top left of the panel. 17
- Figure 8 . Hourly CO₂ dry molar fraction [ppm] at Pasadena (CIT from NOAA ObsPack (2017)) surface station (34.1365°N, 118.1265°W, 10m sampling height) and XCO₂ at TCCON station at the same location [6] showing 9km CHE nature runs: Tier 1 in cyan and two versions of the Tier 2 nature run, using operational ECMWF analysis in red, and ERA-5 re-analysis in yellow. A NASA nature run with GEOS-5 (in blue) and observations (black circles). Triangles show the model data collocated with observations (after application of averaging kernel in lower panel). 17
- Figure 9: Hourly atmospheric column dry molar fraction XCO₂ [ppm] at Sodankyla, Finland (Kivi et al 2017), Garmisch, Germany (Sussman and Rettinger, 2017) and Darwin, Australia (Griffith et al., 2017) from the Tier 1 nature run (cyan), Tier 2 nature run (red), Tier 2 simulation at lower resolution (yellow) and observations (black). The model columns are weighted vertically using the TCCON averaging kernels and priors. Note that Tier 2 stops in July because at the time of writing the deliverable the nature run experiment had not finished. The mean error (δ), standard error (σ) and correlation coefficient (r) are shown at the top left of each panel..... 18
- Figure 10 Hourly atmospheric column dry molar fraction XCH₄ [ppb] at Sodankyla, Finland (Kivi et al 2017) and Garmisch, Germany (Sussman and Rettinger, 2017) and Darwin, Australia (Griffith et al., 2017) from the Tier 1 nature run (cyan), Tier 2 nature run (red), Tier 2 simulation at lower resolution (yellow) and observations (black). The model columns are weighted vertically using the TCCON averaging kernels and priors. Note that the model data stops in October because at the time of writing the deliverable the nature run experiment had not finished. The mean error (δ), standard error (σ) and correlation coefficient (r) are shown at the top left of each panel. 20
- Figure 11 Hourly atmospheric column dry molar fraction XCO [ppb] in July at Sodankyla, Finland (Kivi et al 2017) (upper panel), Garmisch, Germany (Sussman and Rettinger,

2017) (middle panel), and Darwin, Australia (Griffith et al., 2017) (lower panel) from the Tier 1 nature run (cyan), Tier 2 nature run (red) and observations (black). The model columns are weighted vertically using the TCCON averaging kernels and priors. The mean error (δ) and standard error (σ) are shown at the top left of each panel.....	20
Figure 12 XCO ₂ [pm] from the Tier 2 nature run 3-hourly at different TCCON sites (black line) in January : Paris (top panel), Four Corners (middle panel) and Pasadena (lower panel) with the background CO ₂ associated with transport only (dash line) and daily enhancement associated with different emission sectors (energy sector in orange, residential sector in brown, transport sector in magenta, other sectors in purple and biogenic emissions in yellow).....	21
Figure 13 IFS model XCO ₂ (ppm) variability over three TCCON sites for 50-member ensemble for 1-5th* of January (top row) and July (bottom row) from combined model uncertainty (coloured lines). TCCON observations, when available, are shown for the 5 days (black circles). Numbers denote ENS standard error (ppm) after 12, 24, 48 and 96 hours. *Note that values given in text are calculated for whole month. (Adapted from McNorton et al., submitted).....	23
Figure 14 Global standard error of IFS model XCO ₂ (ppm) across 50-member ensemble after a 10-day spin-up. The error represents model transport uncertainty. (Adapted from McNorton et al., submitted).....	24
Figure 15 50-member ENS XCO ₂ (ppm) signal generated by using annual (black) and monthly (blue) uncertainties in anthropogenic emissions divided by the noise from remaining model error over three TCCON sites. (Adapted from McNorton et al., submitted).....	25

Tables

Table 1 Configuration of Tier 1 and Tier 2 simulations	9
Table 2: List of 3D meteorological outputs of the global simulation	11
Table 3: List of 2D meteorological outputs of the global simulation	11
Table 4. Average, minimum and maximum total column model CO ₂ error statistics for the transport model error and the atmospheric response to monthly emission uncertainties (signal), and the signal-to-noise ratio for various emission hotspots for January 2015. Results are calculated from the 50-member IFS ensemble. * Denotes large power stations. (Adapted from McNorton et al., submitted).	25
Table 5: List prescribed surface fluxes used in Tier2 global nature run	31

1 Executive Summary

This report presents the second 9-km global nature run of the CO₂ Human Emission (CHE) project – hereafter referred to as Tier 2 nature run -- with improved transport and emissions. The main purpose of this simulation is to provide a reference global simulation to be performed at the higher operational resolution (9km) as part of the CHE library of simulations. This library of simulations will provide data for observing system simulation experiments (OSSEs) to the CHE consortium and wider scientific community. The configuration of the Tier 2 nature run is based on the Copernicus Atmosphere Monitoring Service (CAMS) CO₂ forecast using the Integrated Forecasting System (IFS) at the European Centre for Medium-range Weather Forecasts (ECMWF), but with improved transport and emissions. The main differences with the Tier 1 CHE nature run are (i) the meteorological analysis, (ii) the model transport is based on the latest version of the NWP model at ECMWF, (iii) the anthropogenic emissions which have upgraded to the latest available EDGARv4.3.2FT2015, (iv) the ocean fluxes with the SOCAT-based ocean fluxes from Jena-Carboscope and (v) a revised bias correction of Net Ecosystem Exchange (NEE).

The meteorological aspects of the nature run have not been evaluated in this report because they are consistent with the ECMWF analysis and short-range forecasts which have been extensively investigated and evaluated in various ECMWF Technical Memoranda.

This report illustrates the capability of the nature run to represent the variability of CO₂ at different scales from seasonal and the inter-hemispheric gradient to regional/local variability of synoptic weather systems and plumes from emission hotspots and the diurnal cycle. Comparison with in situ and total column data shows a realistic variability of CO₂. The systematic errors are in the range of 1 to 2ppm for the total column on monthly timescales and less than 1ppm on global scales at baseline sites. These systematic errors are associated in large part to the prescribed and modelled surface fluxes which are not constrained by observations. The seasonal cycle, synoptic and diurnal cycle are all within the range of observed variability recorded by surface and total column observations. A preliminary evaluation of column-averaged CH₄ and CO also show a realistic representation of variability at synoptic and diurnal time-scales. In addition to the upgrades in the 9-km resolution nature run, the Tier 2 simulations have been performed at lower resolution using an ensemble approach to include information on uncertainties in the fluxes and transport.

2 Introduction

The CHE project has been tasked with providing a library of simulations that can be used as a reference -- referred to as nature run -- in OSSEs for the exploration and design of future space-based carbon observing systems. The nature run presented in this report is an improvement of the first Tier 1 nature run (CHE D4.2) and it is part of the effort to build this library. The focus of the simulation is 2015, giving the opportunity to compare the high-resolution global simulation with GOSAT and OCO-2 satellite data, as well as in situ and Total Carbon Column Observing Network (TCCON) data. The background and scope of this Tier2 nature run in the context of the CHE project are presented below

2.1 Background

A part of the commitment to support climate change policy, the CHE project is addressing the challenges of developing a CO₂ emissions monitoring support capacity. Among these challenges, there is the assessment of the requirements for a future space missions dedicated to the monitoring of CO₂. This assessment needs to be done in the framework of

OSSEs which are based on a reference simulation or nature run used as the truth, from which synthetic observations can be produced. As the nature run is taken to be the truth, the simulation is required to represent a realistic variability of the observed parameters. In this context, the CHE project aims to provide a library of simulations at different scales from global to regional to local, which can be used as nature runs to sample the atmospheric variability associated with regional and local sources/sinks to point sources. The CHE deliverable D2.1 describes the configuration of the different nature runs and their domains/resolutions.

2.2 Scope of this deliverable

The main scope of the Tier2 nature run is to provide boundary conditions to regional models over Europe and Asia, which are an improvement on the previous Tier1 nature runs. The objectives and work done associated with this Tier2 nature run can be found below.

2.2.1 Objectives of this deliverable

The objective of this deliverable is to document the model configuration and the available model output of the CHE Tier2 global nature run. A preliminary evaluation is also provided together with snapshots of atmospheric column-averaged CO₂ that illustrate the detailed structure and realism of the high-resolution global simulation. The complete data set will be submitted to Earth System Science Data (ESSD) (Agusti-Panareda et al., 2019, in preparation).

2.2.2 Work performed in this deliverable

Two year-long global simulations have been performed based on the CAMS CO₂ forecast configuration as part of the CHE library of simulations. This report presents the second, Tier 2, simulation with improved model transport and CO₂ natural fluxes and anthropogenic emissions. A preliminary evaluation is performed with the current data available based on surface and total column observations (note that the Tier 2 simulation is still ongoing). Tier 1 and Tier 2 simulations are compared, and the tagged tracers are used to illustrate their potential capability to identify the anthropogenic emission signal in the atmosphere. An ensemble of simulations at lower resolution are used to estimate the transport error and the sensitivity of the atmospheric anthropogenic emission signal to emission uncertainties.

2.2.3 Deviations and counter measures

There have been no deviations or counter measures required.

3 Model configuration

The CHE Tier 2 global nature run is a 9-km free-running tracer simulation with state-of-the-art IFS model transport based on the CAMS cyclic forecast configuration which provides 3-hourly 3-D fields depicting a realistic seasonal cycle, day-to-day synoptic variability and diurnal cycle throughout the year 2015. Details of the experiment setup and the model output available can be found in the two sections below. The main differences between the CHE Tier 1 and Tier 2 simulations are highlighted in Table 1. Note that the Tier 2 high resolution simulation had not completed the full year at the time this deliverable was written. A lower resolution simulation (25km) with the Tier 2 transport model and new CO₂ anthropogenic and natural fluxes is presented for the full 2015 (see Table 1 for further details).

3.1 Experiment set up

Table 1 Configuration of Tier 1 and Tier 2 simulations

Components	CHE Tier 1 nature run	CHE Tier 2 9km nature run	CHE Tier 2 25km simulation with ensemble
Surface fluxes	Annual EDGARv4.2FT2010 anthropogenic; monthly Takahashi et al. (2009) ocean climatology; CTESSEL biogenic with BFAS (Agusti-Panareda et al., 2016); GFAS fires (Kaiser et al., 2012)	Monthly EDGARv4.3.2 anthropogenic, daily residential heating; monthly Rodenbeck et al. (2013) ocean, CTESSEL biogenic with revised BFAS (Agusti-Panareda et al., 2016), GFAS fires (Kaiser et al., 2012)	Monthly EDGARv4.3.2 anthropogenic, daily residential heating; monthly Rodenbeck et al. (2013) ocean, CTESSEL biogenic with revised BFAS (Agusti-Panareda et al., 2016), GFAS fires (Kaiser et al., 2012)
Meteorological input	Operational ECMWF analysis	ERA-5 reanalysis	Operational ECMWF analysis
Initial conditions	CAMS GHG analysis (20150101)	CAMS re-analysis (20141226)	CAMS GHG analysis (20150101)
Tagged tracers	CO ₂ anthropogenic, biogenic, fires, ocean.	+sectorial anthropogenic emissions (power plants, manufacturing, residential heating, transport, other).	No tagged tracers
Model version	IFS CY43R1	IFS CY46R1	IFS CY46R1
Resolution	9km L137	9km L137	25km L137

The Tier 1 and Tier 2 global nature runs have adopted the same configuration as the CAMS high CO₂ resolution forecast (<https://atmosphere.copernicus.eu/maps/global-carbon-dioxide-forecast>), with 1-day forecasts of atmospheric CO₂, CH₄ and linear CO and all the standard Numerical Weather Prediction (NWP) fields issued every day from 00UTC based on the NWP framework. The meteorological initial conditions of each 1-day forecast come from the ECMWF operational NWP analysis, while the CO₂, CH₄ and linear CO tracers are initialised with the previous 1-day forecast, in a cyclic mode, which means they are essentially free-running fields. The nature run covers the period from 1 January 2015 to 31 December 2015. In the Tier 2 nature run, the initial conditions for CO₂, CH₄ and CO on 26 December 2014 are extracted from the CAMS GHG re-analysis (Inness et al., 2019) instead of the CAMS GHG analysis (Massart et al., 2014, 2016) and CAMS near-real time analysis (Inness et al., 2015) used in Tier 1 (on 1 January 2015). NWP analysis of meteorological fields is one of the main elements determining the quality of the transport (Locatelli et al. 2013). Therefore, ensuring

the meteorological fields are close to the analysis by having a sequence of 1-day forecasts will ensure the transport is as realistic as possible. The tier 2 simulation uses ERA-5 NWP analysis instead of the operational ECMWF NWP analysis to ensure consistency throughout the simulation period.

The tracer transport and CO₂ biogenic fluxes, which are two of the largest contributors to the variability of CO₂ are modelled online in the IFS (Agusti-Panareda et al., 2014 and Agusti-Panareda et al. 2016). The model advection is computed by a semi-Lagrangian scheme (Hortal, 2002; Untch and Hortal, 2006), which is not mass conserving by default. Thus, a mass fixer is required to ensure mass conservation at every time step (Agusti-Panareda et al., 2017). The latest version of the mass fixer is documented in Diamantakis and Agusti-Panareda (2018). The turbulent mixing scheme is described in Beljaars and Viterbo (1998) and Koehler et al. (2011). The convection scheme is based on Tiedtke (1989) (see Bechtold et al., 2008, for further details). Full documentation of the IFS can be found in <https://www.ecmwf.int/en/forecasts/documentation-and-support/changes-ecmwf-model/ifs-documentation>. The CO₂ emissions from land vegetation are modelled online using the CTESSEL Carbon module integrated in the land surface model of the IFS (Boussetta et al., 2013). The fluxes have been evaluated with FLUXNET data and compared to different models (e.g. CASA and ORCHIDEE) with a comparable performance on synoptic to seasonal scales (Balzarolo et al., 2014). An online bias correction scheme (Agusti-Panareda et al., 2016) is applied to the modelled Gross Primary Production (GPP) and ecosystem respiration (Reco) fluxes to correct for biases in the Net Ecosystem Exchange (NEE) budget compared to a climatology of optimized fluxes (Chevallier et al., 2010). The biogenic flux bias correction has been updated for consistency with the new anthropogenic emissions.

All the tracer surface fluxes, excluding the biogenic CO₂ fluxes from land, are prescribed (see Table 5 in Annex). The prescribed emissions in the Tier 2 nature run have been improved to the latest EDGARv4.3.2FT2015 data (Janssens-Maenhout et al., 2019, CHE D3.3) with monthly mean variation from EDGAR v4.2FT2010 and 7 groups of emission sectors (CHE D3.3). While Tier 1 nature run used annual mean emissions from the EDGAR v4.2FT2010 (Olivier and Janssens—Maenhout, 2012) for CO₂ and CH₄ and CAMS MACCity emissions (Granier et al., 2011) for CO, which contain no day-to-day variability in these prescribed emissions. For these tier2 simulations, anthropogenic and biogenic emissions for CO have a month-to-month variation and CH₄ also has a seasonal cycle for the emissions from rice paddies. The wetland CH₄ emissions are from a climatology of LPJ-HYMN data set (Spanhi et al. 2011) with an original resolution of 1x1 degree.

Because the IFS is a state-of-the-art operational NWP model, the meteorological fields of each model version are extensively evaluated. The IFS model version used in the Tier 1 nature run was CY43R1, which was operational weather forecast model at ECMWF from 22 November 2016 to 10 July 2017. While Tier 2 was upgraded to use the current operational model version (CY46R1) at ECMWF, implemented on 11 June 2019. A full evaluation of the CY46R1 model can be found in Buizza et al. (2018) and Tier 1 CY43R1 evaluation in Haiden et al. (2017).

The 9km simulation is based on a new model grid (Malardel et al. 2016) used in the current operational NWP forecast at ECMWF which comprises up to 904 million model grid points, 137 levels and a time step of 7.5 minutes.

3.2 Model output

As with the Tier 1 simulation, the Tier 2 global nature run will be used as boundary conditions to the WP2 regional models, and therefore there are several meteorological and tracer 2D and 3D fields that need to be provided as model output. A list of the required model outputs necessary for the nesting of the other simulation domains have been provided by the WP2 partners (see Tables 2 and 3). Additionally, the CO₂ and CH₄ surface fluxes and the experimental tagged tracers have also been archived as model output which may be useful for other applications (e.g. global OSSEs).

The output fields are provided as 3-hourly data with a maximum horizontal resolution of 0.1x0.1 degree on a regular latitude/longitude grid. The data can be accessed via ECMWF MARS archiving system: experiment ID is “ha58” (stream=OPER, class=RD). The data will also be available from the Copernicus Climate Data Store at the end of 2020. Users can also contact Copernicus User Support (copernicus-support@ecmwf.int) to make enquiries about data access.

Table 2: List of 3D meteorological outputs of the global simulation

Variable name	Variable abbreviation
Specific humidity	Q
Temperature	T
Pressure	P
Wind components	U,V
Cloud liquid water content	CLWC
Cloud ice water content	CIWC

Table 3: List of 2D meteorological outputs of the global simulation

Variable name	Variable abbreviation
Geopotential and land mask	Z/LSM
Snow depth	SD
Snow temperature	TSN
Skin temperature	SKT
Skin Reservoir Content	SRC
Soil temperature	STLi
Soil wetness	SWLi
Logarithm of surface pressure	LNSP
Mean sea-level pressure	MSL
Sea-ice cover	CI
Sea surface temperature	SSTK
10 metre wind components	10U, 10V
2 metre temperature	2T
2 metre dewpoint temperature	2D

3D tracers

- CO₂ [kg/kg]
- CO [kg/kg]
- CH₄ [kg/kg]

Conversion of units from kg/kg to dry molar fraction in ppm requires the application of the conversion factor $f=10^6 \times M_{air}/M_{tracer}$, where M_{air} and M_{tracer} are the molar masses of dry air and tracer respectively.

2D tracers

- XCO₂ [ppm] (tcco2)
- XCH₄ [ppb] (tcch4)
- TCCO [kg/m²] (tcco)

Surface fluxes

- NEE [kg m⁻²s⁻¹] archived as instantaneous flux (fco2nee) or accumulated (aco2nee). Note that positive values are associated with a sink and negative values with a source (following IFS convention).
- CO₂, CH₄ and CO fire emissions [kg m⁻²s⁻¹] (co2fire/ch4fire/cofire with positive values indicating a source).
- CO₂ anthropogenic emissions [kg m⁻²s⁻¹] (co2apf with negative values indicating a source following IFS convention).
- CO₂ ocean fluxes [kg m⁻²s⁻¹] (co2of with negative/positive values corresponding to source/sink following IFS convention).
- CH₄ total emissions excluding fires [kg m⁻²s⁻¹] (ch4f with negative/positive values indicating source/sink following IFS convention).
- Note that anthropogenic emissions for CO are not archived, but the prescribed emissions will be made available to users (positive values indicate source).

Tagged tracers

Tagged tracers associated with different emissions (e.g. anthropogenic, biogenic, fires, oceans) are also provided by using a flux-denial configuration, where extra tagged tracers are initialised with the realistic tracer fields, but they are evolving without the influence of a specific (tagged) emission sector during the 1-day forecast. The pattern of enhancement associated with that specific emission sector during the 1-day forecast can then be obtained by subtracting the flux-denial tracer from the full tracer (with all the emissions sectors). The sum of all the enhancements from the different fluxes add up to the enhancement of the total flux, thus showing that the assumption of linearity in the transport also holds in the IFS model. Tier 2 has introduced specific tagged tracers for the seven anthropogenic emission groups described in CHE D3.3 (i.e. average power stations, super power stations, manufacturing, transport, residential, aviation and others).

4 Atmospheric tracer variability on seasonal, synoptic and diurnal scales

The global nature run displays the variability of CO₂ at different scales, from seasonal large-scale patterns such as the gradients between southern and northern hemispheres (Figure 1), to zonal gradients associated with synoptic weather systems (Figure 2). The high resolution can also add to the detail and intricacies of the mesoscale variations and the plumes emanating from point sources. For example, the CO₂ plumes from Paris and Moscow as well as some power stations in Germany are clearly visible from Figure 2.

The complex distribution associated with distinct weather patterns, such as extratropical cyclones coming from western Europe with their upper level troughs behind them can mask the small-scale variability associated with plumes from point sources. For example, the lower

CO₂ associated with a stratospheric intrusion behind a low-pressure system can mask signal of a plume near the surface in the total column CO₂ (XCO₂) plots. The tagged tracers in the nature run provide information on the CO₂ enhancement associated with the local emissions and therefore highlight the location of the plumes coming from the various hotspots (see Figure 3).

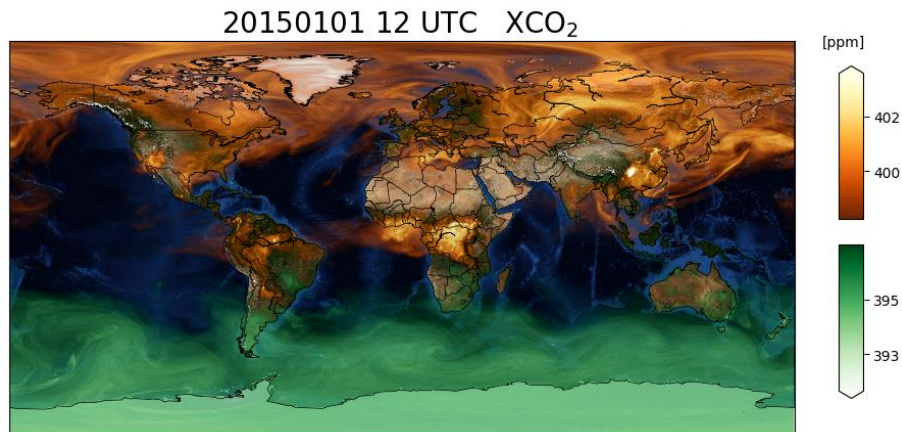


Figure 1 XCO₂ [ppm] spatial distribution on 1 January 2015 12 UTC. Values above and below the global mean in reds and greens respectively (see colour bar).

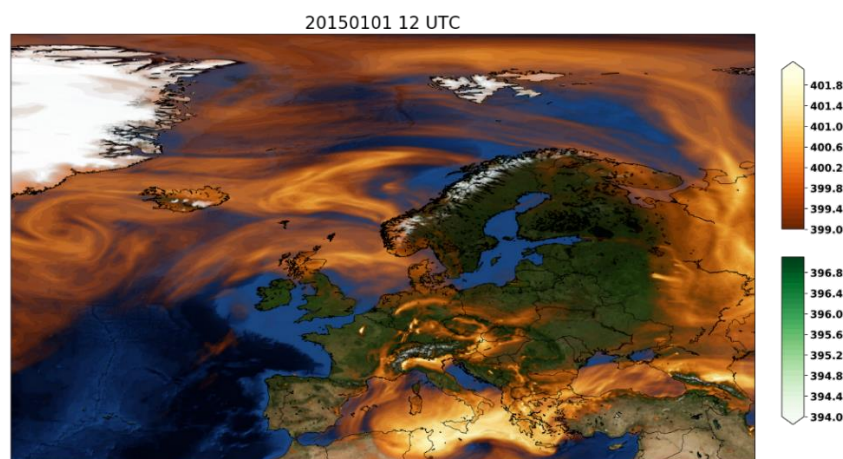


Figure 2 XCO₂ [ppm] spatial distribution on 1 January 2015 12 UTC over Europe. Values above and below the global mean in reds and greens respectively (see colour bar).

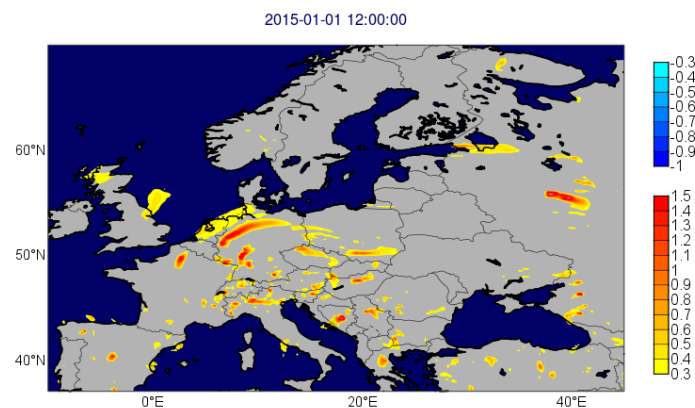


Figure 3 XCO₂ enhancement and depletion (see colour bar in ppm) associated with the total CO₂ flux at the surface (i.e. anthropogenic and biogenic) on 01 January 2015 after 12 hours of

simulation in the CHE Tier2 9km nature run. Light blue colour show CO₂ depletion associated with natural sinks and yellow/red colours show enhancement associated with CO₂ sources.

Plumes from hotspots can be studied with tracers tagged to different emission sources and natural fluxes (section 4.1). A range of observations have been used to evaluate the realism of the nature run at seasonal, synoptic and diurnal timescales at the surface (section 4.2) and the total atmospheric column (section 4.3). The tagged tracers can be used to interpret the peaks in XCO₂ by attributing the atmospheric XCO₂ anomalies to an enhancement/depletion associated with local emissions/sinks or advection (section 4.4).

4.1 Plumes

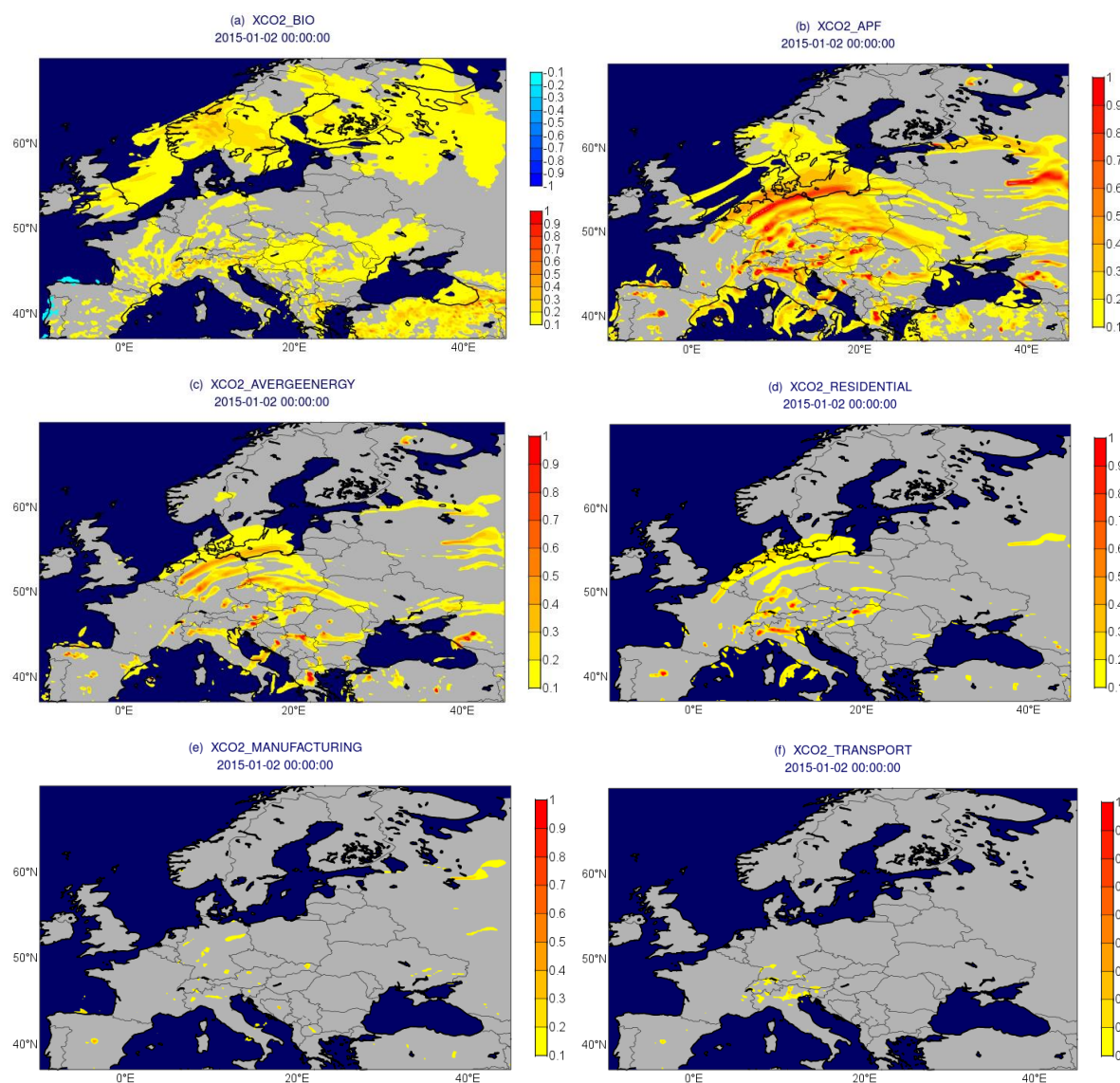


Figure 4 XCO₂ enhancement and depletion (see colour bar in ppm) associated with (a) biogenic fluxes; (b) total anthropogenic emissions; (c) average power stations (excluding super power stations); (d) residential heating, (e) industry/manufacturing; and (f) transport (excluding aviation) on 02 January 2015 after 24 hours of simulation in the CHE Tier2 9km nature run.

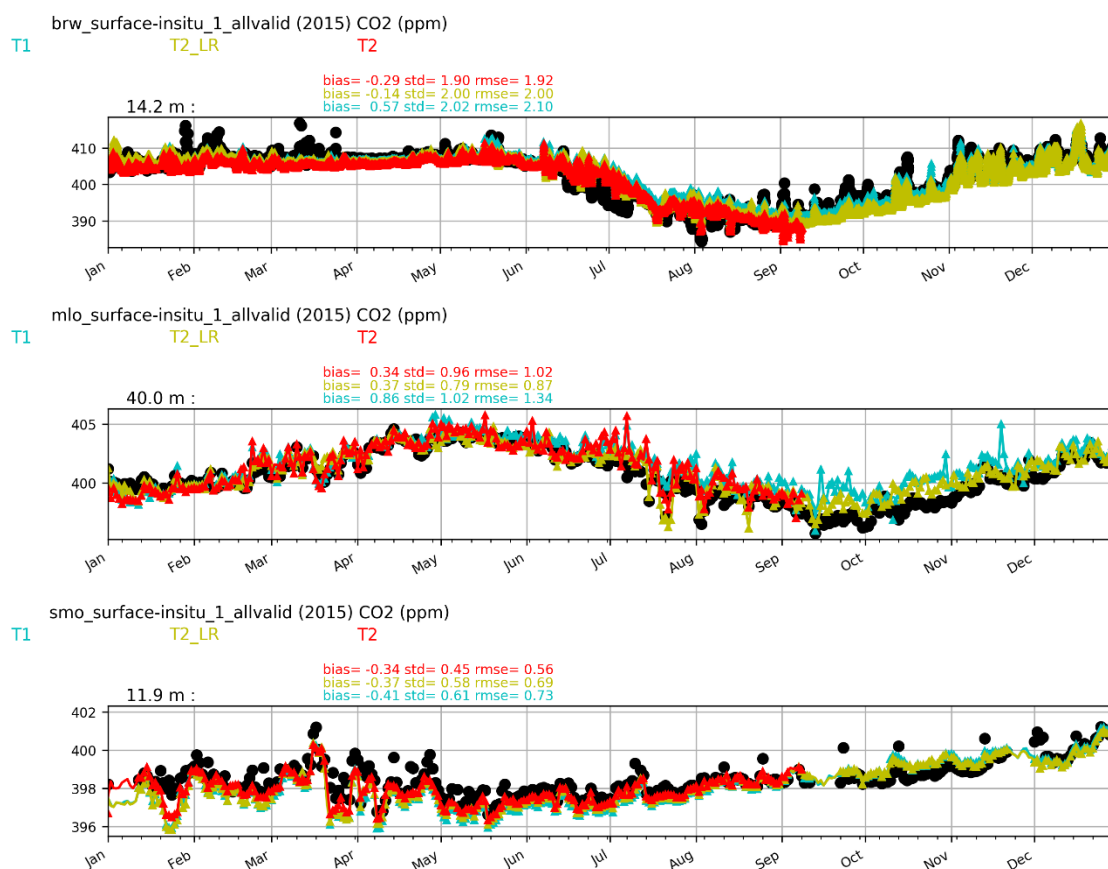
One of the aims of the CO₂ Monitoring Verification System is to monitor hotspots by measuring their associated plumes downstream. These plumes are often superimposed with larger-scale anomalies of biogenic origin and the transport of regional anomalies by synoptic weather systems. Figure 4 illustrates the signal from the local enhancements over Europe. Some emissions will not be detected by satellites if their atmospheric enhancement is less

than 0.3ppm. The XCO₂ enhancement depends on the flux intensity and on the wind speed. Point sources such as power stations have well defined plumes which can be easily seen, though some are also below the detection threshold of satellites (e.g. plumes over the UK have an enhancement between 0.1 and 0.2 ppm). Biogenic fluxes are generally weak and positive in the winter. On this specific day (from 1 January 00UTC to 2 January 00UTC) the XCO₂ biogenic enhancement is mostly below 0.3ppm and the emission sectors from Industry/manufacturing and transport also show a weak signal close to 0.1ppm.

4.2 Surface variability

The inter-hemispheric gradient and the seasonal cycle of CO₂ are depicted in Figure 5 by the baseline National Oceanic and Atmospheric Administration (NOAA) observatories at Barrow (Alaska, USA), Mauna Loa (Hawaii, USA), Samoa and South Pole. Although the amplitude of the seasonal cycle is slightly underestimated, the biases of the background air are less than 1ppm (Figure 5).

Tier 2 and tier 1 CO₂ simulations are consistent, with tier 2 showing some improvement in the seasonal cycle of surface CO₂. Tier 2 also has a large reduction in the bias of surface CH₄ in the tropics of approximately 20 ppb (Figure 6). This is associated with the change of initial conditions from CAMS analysis in Tier 1 to the CAMS re-analysis in Tier 2 (as described in Table 1).



CO₂ HUMAN EMISSIONS 2019

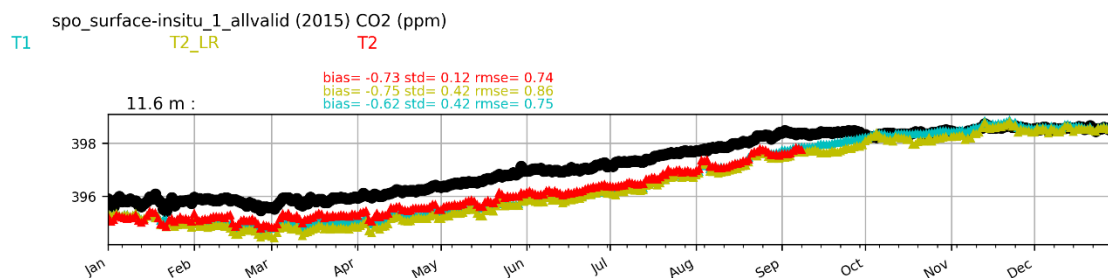


Figure 5: Daily mean surface CO₂ at four NOAA baseline stations: brw (Barrow, Alaska, USA), mlo (Mauna Loa, Hawaii, USA at 71.3°N 156.6°W, 11 m a.s.l), smo (Tutuila, American Samoa, USA at 14.25°S 170.6°W, 42 m a.s.l), spo (South Pole, Antarctica at 89.9°S 24.8°W, 2810 m a.s.l) from the Tier 1 nature run (blue), Tier 2 nature run (red), Tier 2 simulation at lower resolution (yellow) and observations (black). The observations have been obtained from the NOAA ObsPack (2017). The bias, standard error and root mean square error (rmse) are shown at the top of each panel, together with the sampling height [m] for each station. Note that Tier 2 stops in July because at the time of writing the deliverable the nature run experiment had not finished. The station sampling height is provided on the top left of each panel.

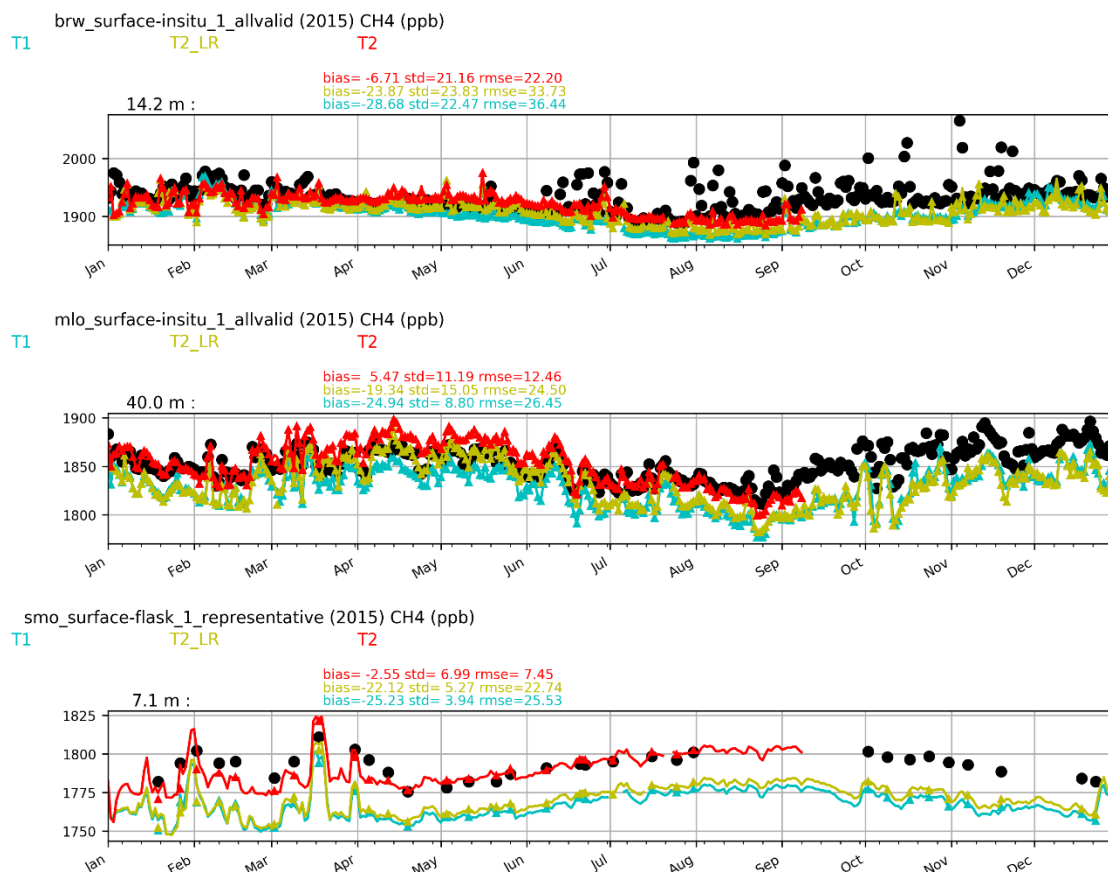


Figure 6 Daily mean surface CH₄ at three NOAA baseline stations: brw (Barrow, Alaska, USA), mlo (Mauna Loa, Hawaii, USA at 71.3°N 156.6°W, 11 m a.s.l), smo (Tutuila, American Samoa, USA at 14.25°S 170.6°W, 42 m a.s.l) from the Tier 1 nature run (blue), Tier 2 nature run (red), Tier 2 simulation at lower resolution (yellow) and observations (black). The observations have been obtained from the NOAA ObsPack (2017). The bias, standard error and root mean square error (rmse) are shown at the top of each panel, together with the sampling height [m] from each station. Note that Tier 2 stops in July because at the time of writing the deliverable the nature run experiment had not finished. The station sampling height is provided on the top left of each panel.

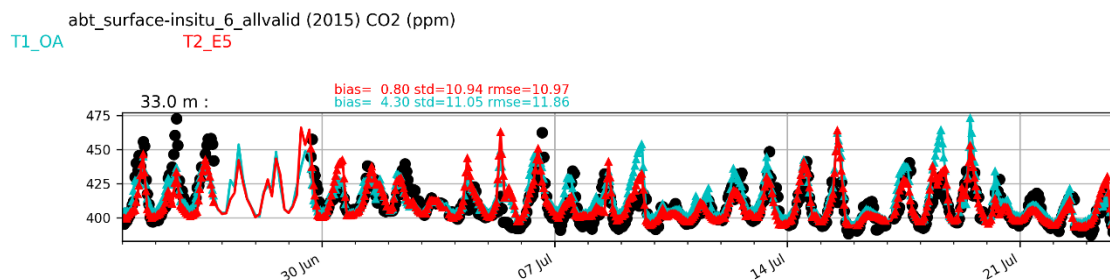


Figure 7: Hourly surface CO₂ at three in situ stations in North America: abt (Abbotsford, British Columbia, Canada at 49.03°N 122.37°W and 100m a.s.l, Environment Canada) from the Tier 1 nature run (T1_OA, blue), Tier 2 nature run (T2_EA, red) and observations (black) in July 2015. The observations have been obtained from the NOAA ObsPack (2017). The bias, standard error and root mean square error (rmse) are shown at the top of each panel, together with the sampling height [m] for each station. The station sampling height is provided on the top left of the panel.

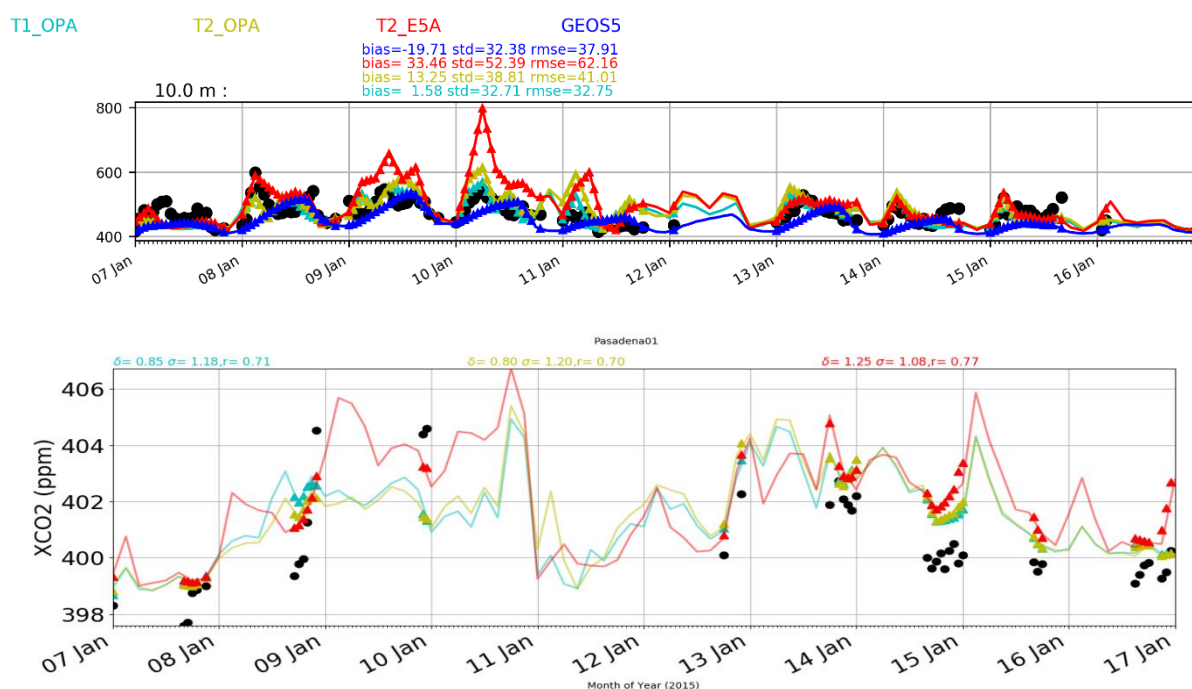


Figure 8 . Hourly CO₂ dry molar fraction [ppm] at Pasadena (CIT from NOAA ObsPack (2017)) surface station (34.1365°N,118.1265°W, 10m sampling height) and XCO₂ at TCCON station at the same location [6] showing 9km CHE nature runs: Tier 1 in cyan and two versions of the Tier 2 nature run, using operational ECMWF analysis in red, and ERA-5 re-analysis in yellow. A NASA nature run with GEOS-5 (in blue) and observations (black circles). Triangles show the model data collocated with observations (after application of averaging kernel in lower panel).

The amplitude of the diurnal cycle is generally well captured, as well as its day-to-day variation with synoptic conditions (Figures 7 and 8). It is worth noting that the online modelling of the biogenic CO₂ fluxes over land contributes to the pronounced diurnal cycle

with photosynthesis uptake during the day and ecosystem respiration during the night time, in addition to the diurnal cycle associated with the boundary layer mixing (Agusti-Panareda et al., 2014). For sites close to emission hotspots, like Pasadena, the meteorological analysis - whether operational ECMWF analysis of ERA-5 re-analysis - appears to be as important as the difference between the Tier 1 and Tier 2 emissions in the atmospheric CO₂ and XCO₂ variability (Figure 8).

4.3 Total column variability

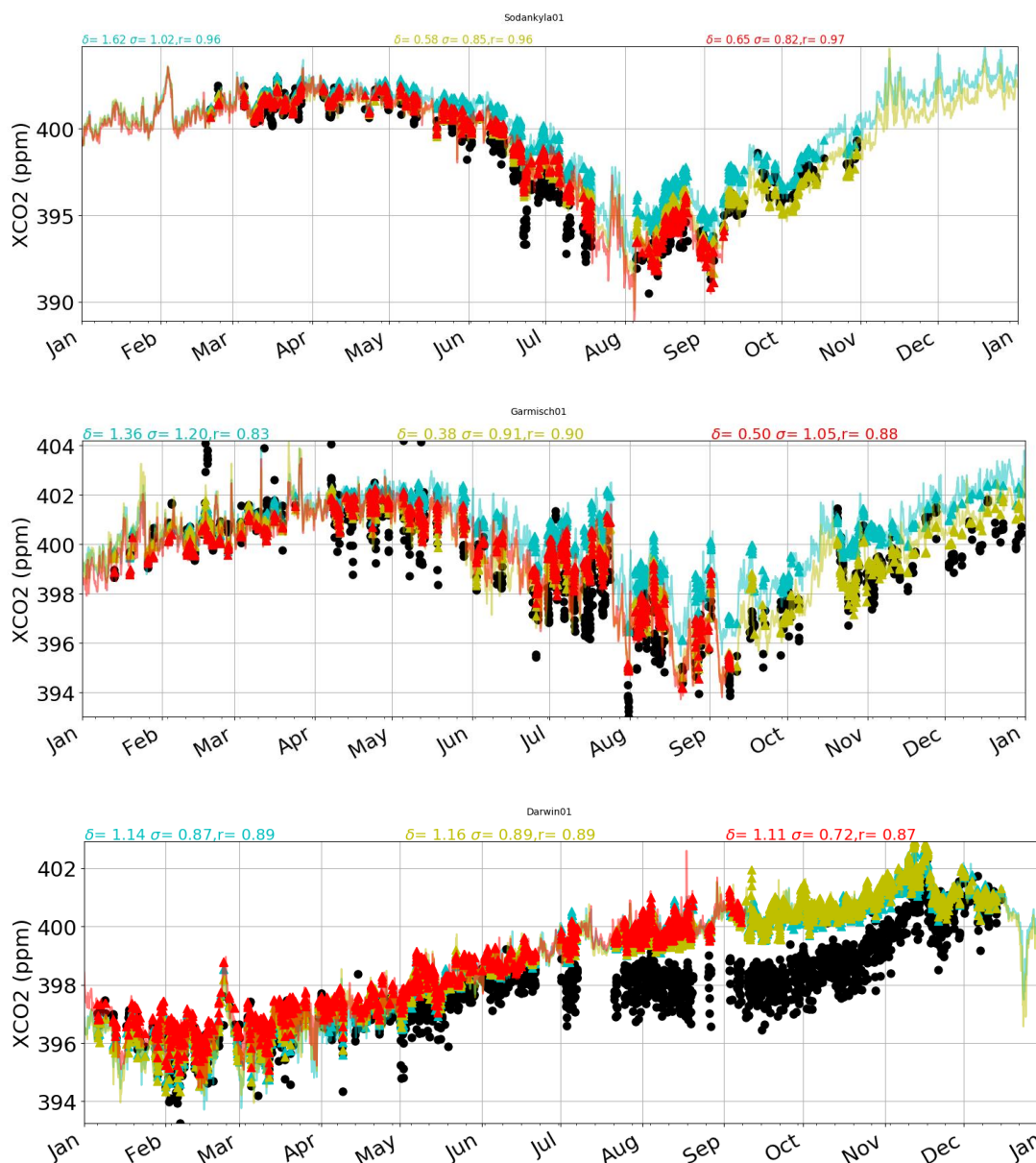


Figure 9: Hourly atmospheric column dry molar fraction XCO₂ [ppm] at Sodankyla, Finland (Kivi et al 2017), Garmisch, Germany (Sussman and Rettinger, 2017) and Darwin, Australia (Griffith et al., 2017) from the Tier 1 nature run (cyan), Tier 2 nature run (red), Tier 2 simulation at lower resolution (yellow) and observations (black). The model columns are weighted vertically using the TCCON averaging kernels and priors. Note that Tier 2 stops in July because at the time of writing the deliverable the nature run experiment had not finished. The mean error (δ), standard error (σ) and correlation coefficient (r) are shown at the top left of each panel.

The averaged atmospheric column dry molar fraction is also evaluated using observations at TCCON sites (Wunch et al., 2010) that cover the interhemispheric gradient. For XCO₂, the standard error of daily mean model data is around 1 ppm, while the bias ranges between 1 and 2ppm, with largest errors during the growing season when the biogenic fluxes are most active. The amplitude of the seasonal cycle at high mid-latitudes is underestimated by 1 to 2ppm, but there is a significant improvement of around 1ppm with respect to Tier 1 (Figure 9). The synoptic day-to-day variability is well captured and it is consistent between Tier 1 and Tier 2, except for some significant differences close to emission hotspots like Pasadena (Figure 8, lower panel).

For XCH₄, there is a general positive bias ranging from a few ppb to 25ppb at high latitudes, with a large reduction of the bias in the tropics (Fig. 10). The bias can be largely explained by the initial conditions of the nature run (i.e. CAMS analysis or CAMS re-analysis) as shown in Figure 10. The synoptic variability is well represented by the model with a standard error generally lower than 12ppb. The diurnal and synoptic variability is also well captured for XCO (Figure 11).

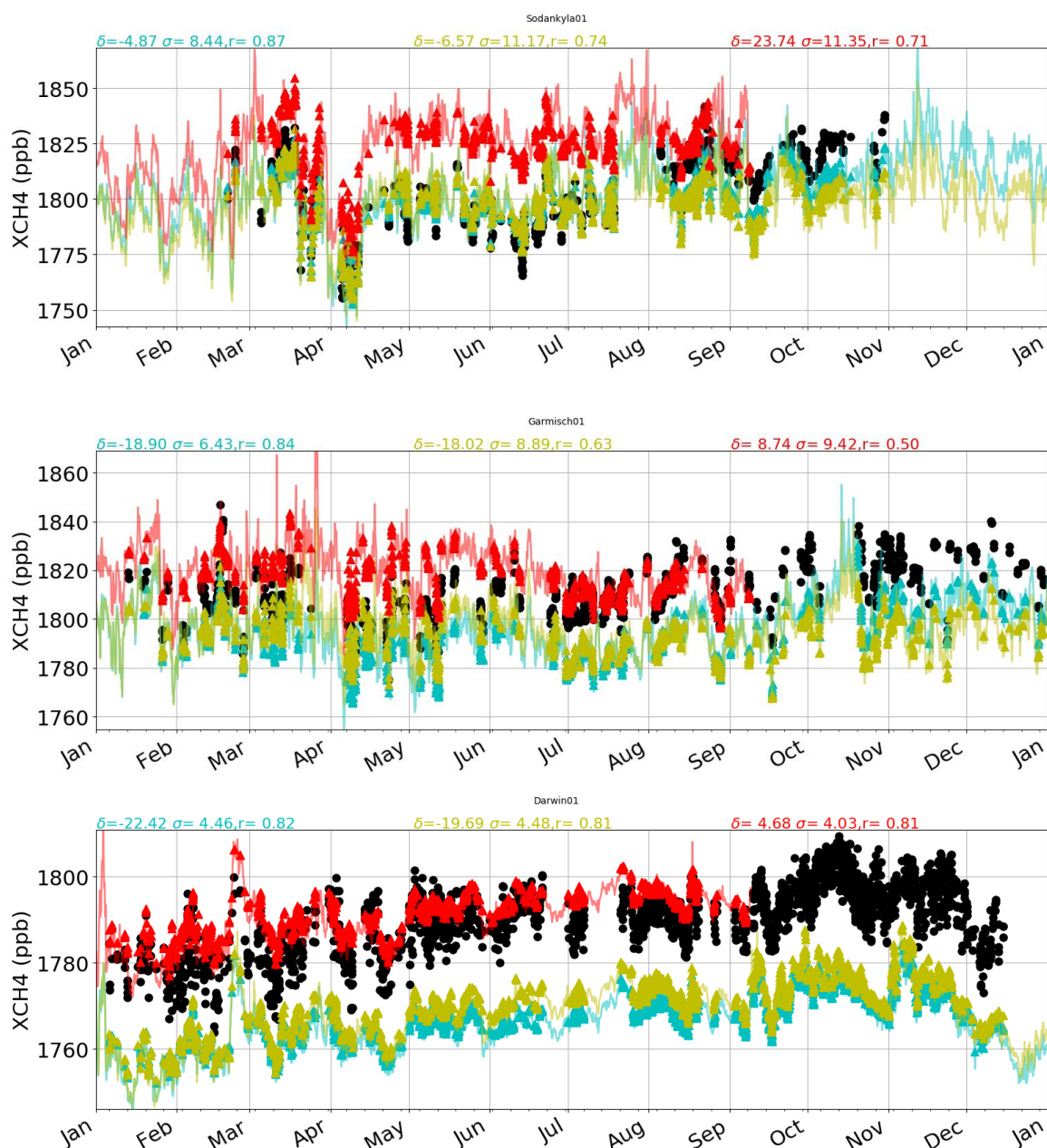


Figure 10 Hourly atmospheric column dry molar fraction XCH_4 [ppb] at Sodankyla, Finland (Kivi et al 2017) and Garmisch, Germany (Sussman and Rettinger, 2017) and Darwin, Australia (Griffith et al., 2017) from the Tier 1 nature run (cyan), Tier 2 nature run (red), Tier 2 simulation at lower resolution (yellow) and observations (black). The model columns are weighted vertically using the TCCON averaging kernels and priors. Note that the model data stops in October because at the time of writing the deliverable the nature run experiment had not finished. The mean error (δ), standard error (σ) and correlation coefficient (r) are shown at the top left of each panel.

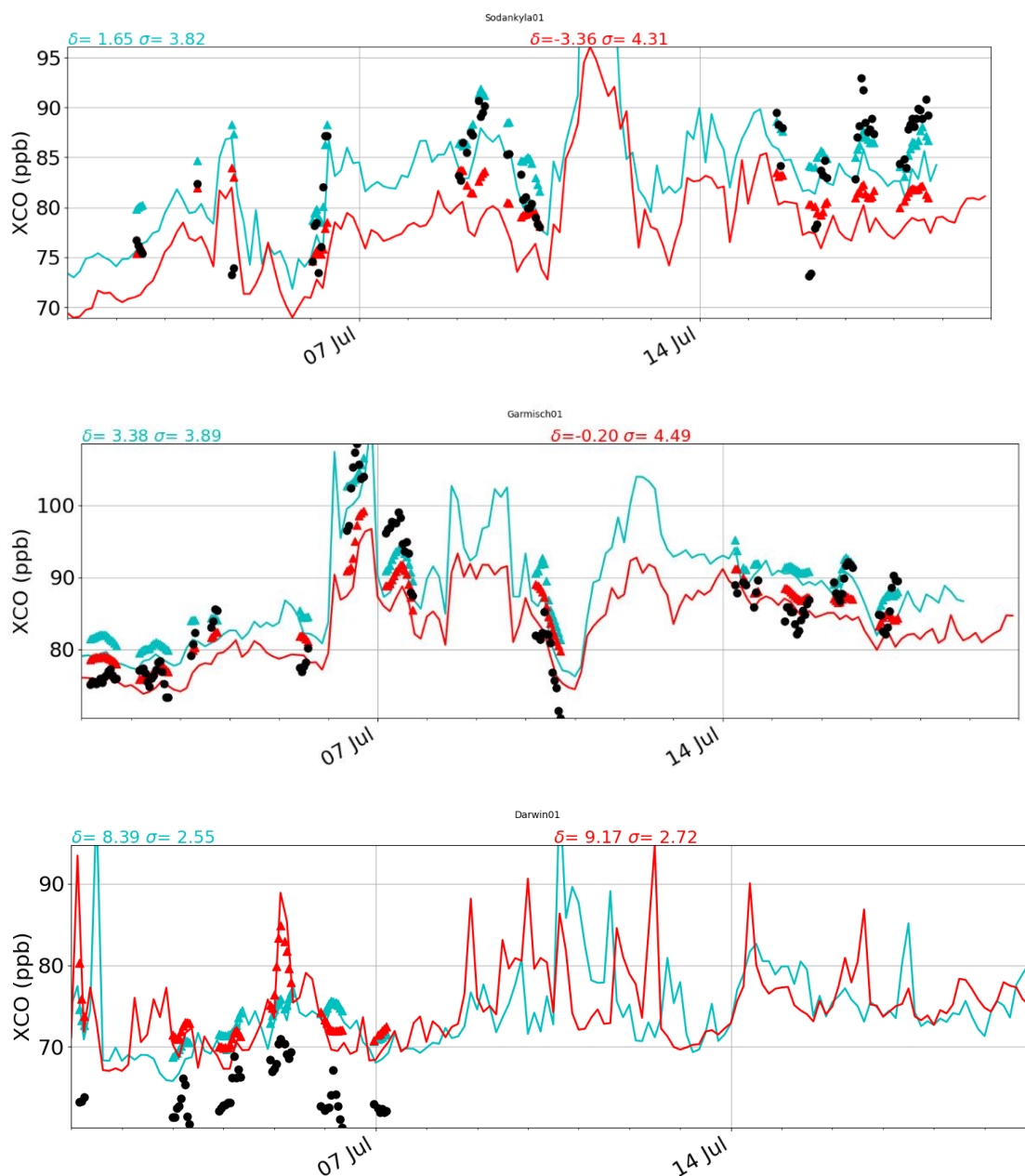


Figure 11 Hourly atmospheric column dry molar fraction XCO [ppb] in July at Sodankyla, Finland (Kivi et al 2017) (upper panel), Garmisch, Germany (Sussman and Rettinger, 2017) (middle panel), and Darwin, Australia (Griffith et al., 2017) (lower panel) from the Tier 1 nature run (cyan), Tier 2 nature run (red) and observations (black). The model columns are weighted vertically using the TCCON averaging kernels and priors. The mean error (δ) and standard error (σ) are shown at the top left of each panel.

4.4 Interpreting total column variability with tagged tracers

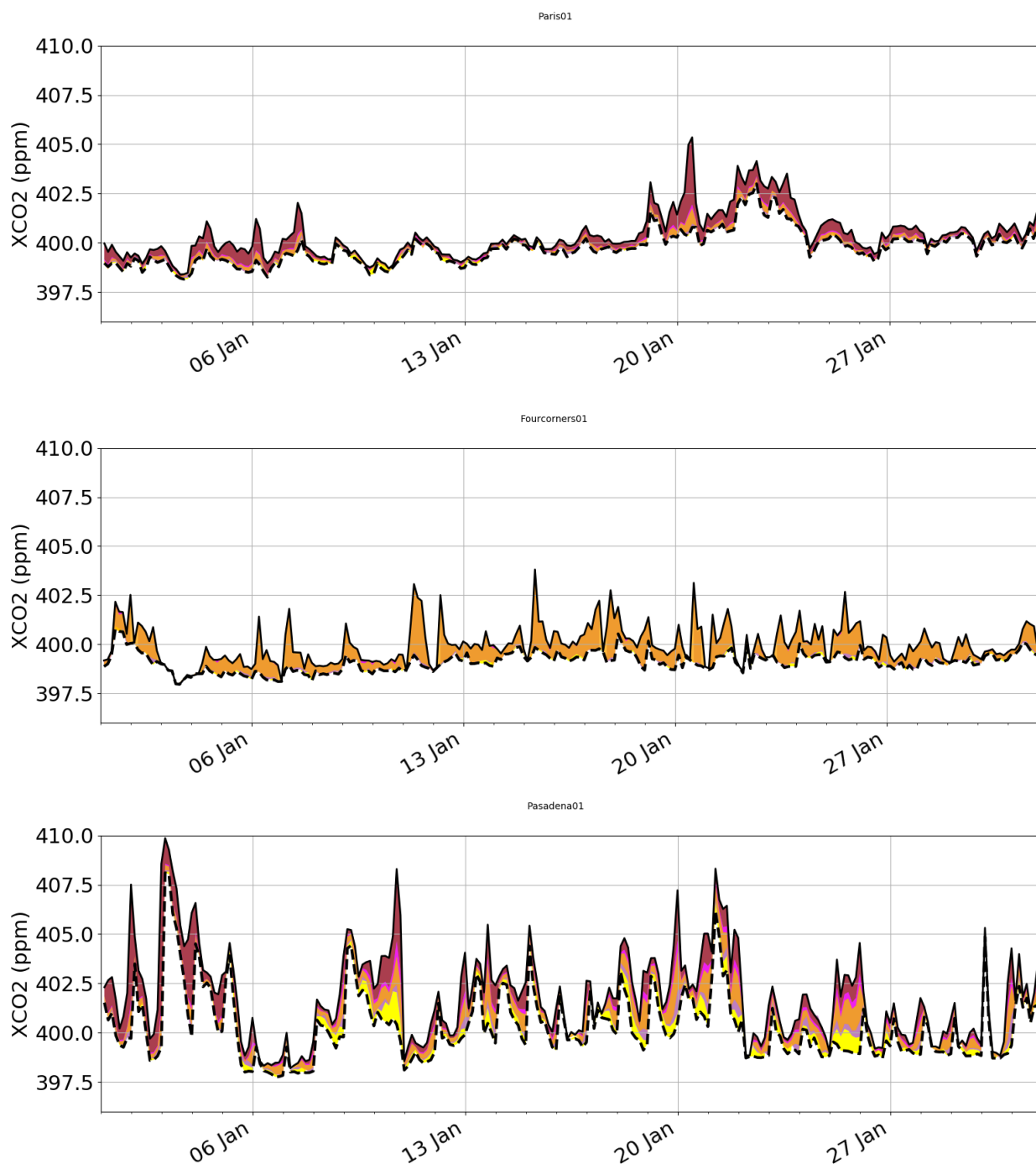


Figure 12 XCO₂ [ppm] from the Tier 2 nature run 3-hourly at different TCCON sites (black line) in January : Paris (top panel), Four Corners (middle panel) and Pasadena (lower panel) with the background CO₂ associated with transport only (dash line) and daily enhancement associated with different emission sectors (energy sector in orange, residential sector in brown, transport sector in magenta, other sectors in purple and biogenic emissions in yellow).

To distinguish the XCO₂ signal from transport from the local emissions, Figure 12 compares the XCO₂ (solid line) with a tracer that is initialised with the same XCO₂ every day at 00UTC but does not include any emissions during the 24-hour period, just transport (dash line).

Most TCCON stations have the two lines superimposed, which means that they are not influenced by local emissions. However, TCCON stations close to emission hotspots (e.g. Paris, Four Corners and Pasadena) have a strong influence from local emissions. The tagged tracers in the Tier 2 CHE global nature provide information on the enhancement each day from 00 UTC associated with the different anthropogenic emission sectors. For example, in Paris the XCO₂ peaks are mostly associated with residential combustion (e.g. 19 and 20 January). While in Four Corners samples the local emissions from a nearby coal-fired power plant as shown by the XCO₂ peaks matching the regular XCO₂ enhancement associated with the energy sector. Finally, Pasadena shows a mixture of influences. All emission sectors (i.e. biogenic, transport, energy production and residential heating) and the advection of background CO₂ are important to explain the pronounced XCO₂ variability observed in Pasadena.

5 Ensemble simulations

The CHE Tier 2 simulations include a 25-km free-running 50-member ensemble, which is broadly consistent with the higher resolution nature simulation. Simulations provide 3-hourly global 3-D fields of CO₂ at 137 levels for January 2015. These simulations can be used to quantify uncertainties in initial atmospheric meteorology, uncertainties in model physical tendencies and the spread in the biogenic fluxes as a response to these uncertainties. Anthropogenic uncertainties from WP3.3 are used to perturb emissions and are used to derive a signal-to-noise ratio for a perspective CHE prototype. Several experimental configurations have been tested and are reported on in McNorton *et al.* (submitted).

Ensemble simulations were performed using The ENSEMBLE (ENS) component of the IFS, detailed in Leutbecher and Palmer (2008), which used initial conditions inherited from an operational Ensemble Data Assimilation (EDA) component of the IFS. Within this system, uncertainty is accounted for by perturbing assimilated observations using stochastic noise based on a given observation error (Isaksen *et al.*, 2010). In addition to this, both the ENS and the EDA (used to initialise the ENS), use a Stochastically Perturbed Parameterisation Tendencies (SPPT) scheme to represent errors caused by uncertainty in physical parameterisations (Buizza *et al.*, 1999; Leutbecher *et al.*, 2017). The techniques used to represent model error using an online system are well established within the NWP community and these simulations show how they can be adopted by the atmospheric trace gas community. Each month-long ensemble member is comprised of 24-hour forecasts reinitialised from the operational EDA, with the 3-D CO₂ field cycled from the last timestep of the previous forecast. As a result, on the first day of the month the ensemble does not include a representation of the initial atmospheric 3-D CO₂ uncertainty; however, the error in initial CO₂ concentrations for each forecast is established within the ensemble after a few days.

Combined model uncertainty from initial conditions, model physical tendencies, biogenic feedback to meteorological uncertainty and anthropogenic emissions, has been validated using TCCON observations. This combined ENS estimated uncertainty, using monthly anthropogenic uncertainties, accounts for between 21% and 65% of total uncertainty (Fig. 13). Larger uncertainties are identified over Caltech because of large local emission gradients. This can lead to an accumulation of atmospheric CO₂ over Caltech in some simulations, whilst the emissions are transported away from the source in others. Around Tsukuba increased biogenic fluxes cause large emission gradients in July, leading to an increased error. Other factors, such as local orography and transport variability, account for the differences seen at each site. The remaining uncertainty likely originates from other sources, such as observation, numerical and representation errors, and structural errors in the biogenic model.

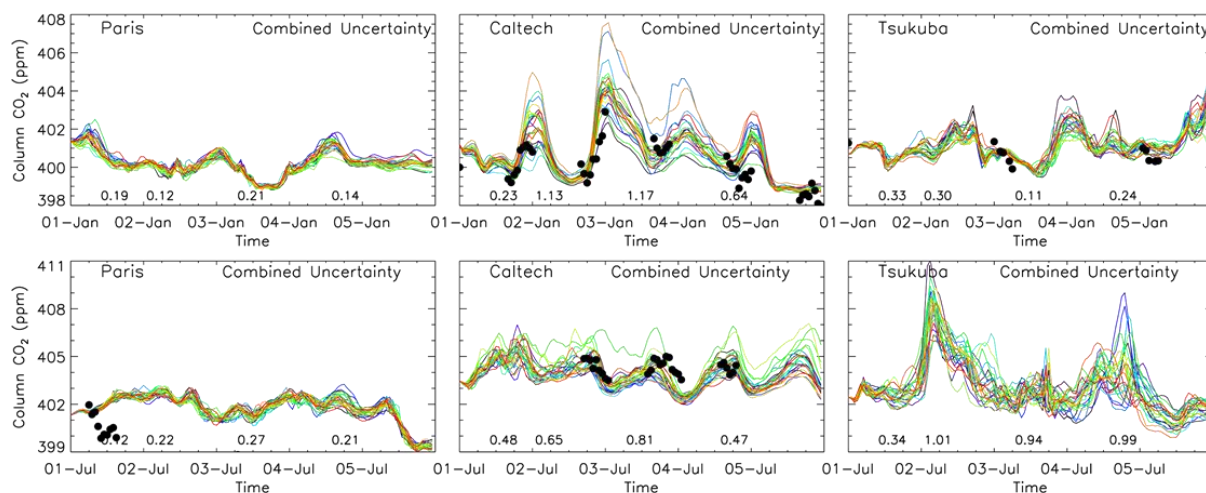


Figure 13 IFS model XCO₂ (ppm) variability over three TCCON sites for 50-member ensemble for 1-5th* of January (top row) and July (bottom row) from combined model uncertainty (coloured lines). TCCON observations, when available, are shown for the 5 days (black circles). Numbers denote ENS standard error (ppm) after 12, 24, 48 and 96 hours. *Note that values given in text are calculated for whole month. (Adapted from McNorton *et al.*, submitted).

5.1 Transport uncertainty estimates

The model transport uncertainty is quantified using a range of initial atmospheric conditions and utilising model perturbations to capture uncertainty in the modelled representation of atmospheric physics. The 50-member ensemble provides an estimated probability distribution function (PDF) of uncertainty. By fixing the emissions of each ensemble member the PDF contains only transport model uncertainty. In a CHE prototype this component would be considered as noise.

XCO₂ transport errors over emission hotspots are found to range between 0.1 and 0.8 ppm, this further increases to 1.7-7.2 ppm for near-surface concentrations. The model transport uncertainty is time and location dependant (Fig. 14), suggesting previous simplified representations of model error fail to provide suitable estimations and flow-dependent patterns should be considered.

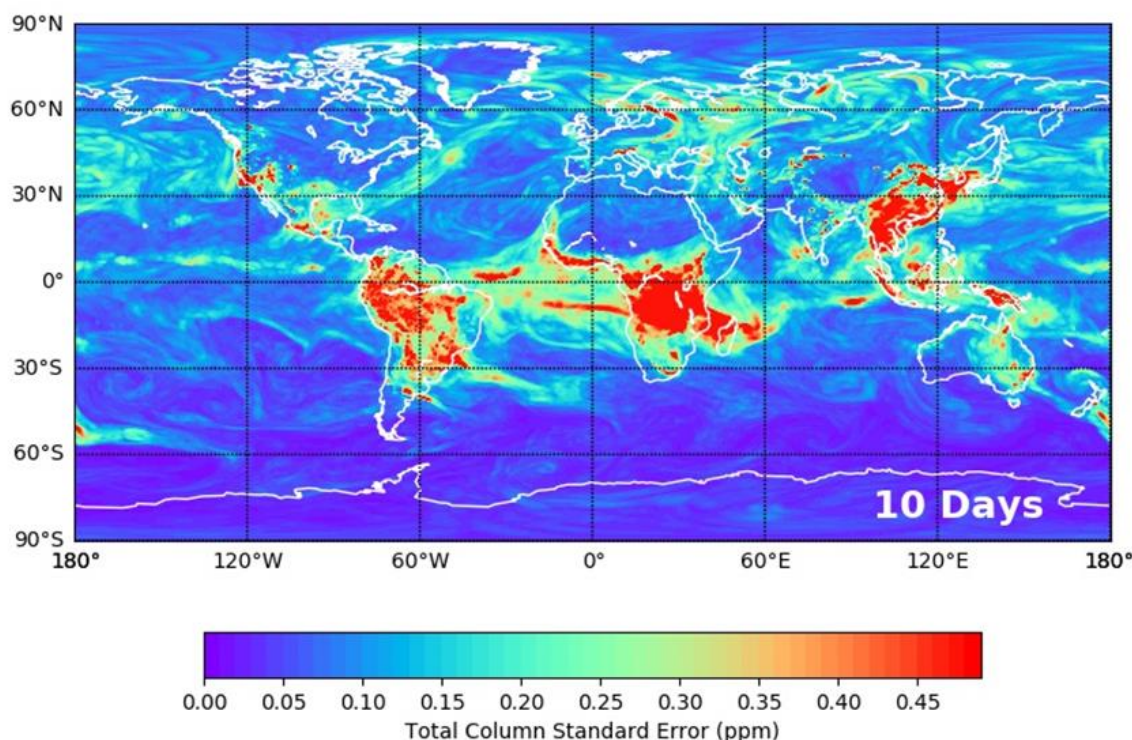


Figure 14 Global standard error of IFS model XCO₂ (ppm) across 50-member ensemble after a 10-day spin-up. The error represents model transport uncertainty. (Adapted from McNorton et al., submitted).

5.2 Sensitivity to anthropogenic emissions

The ratio between the atmospheric XCO₂ signal generated by the prior flux uncertainty (signal) and the remaining model uncertainty (noise), provides a representation on where information can be gained by a future CHE prototype inversion system. Anthropogenic perturbations for tier-2 ensemble simulations were applied using uncertainties calculated in WP 3.3. Anthropogenic emissions were grouped into 7 sectors and log-normal uncertainty assumptions, based on IPCC guidelines (IPCC, 2006), are applied to random noise per country per sector assuming perfect correlation through time and space for a given country and sector.

The uncertainties used to derive a signal are thought to be relatively modest considering they are monthly uncertainties being used at higher temporal scales. Data availability currently restricts the derivation of anthropogenic uncertainties at the required short timescales. For example, daily uncertainties, which would be required for high temporal frequency flux inversions, are expected to be considerably larger than monthly uncertainties. This would provide, in principle a larger signal. Additionally, a lack of prior information prevented the consideration of uncertainty correlations in prior fluxes. Finally, the diurnal variability in emissions, which is likely to influence the modelled atmospheric response to anthropogenic emissions, is not considered. The missing information in prior uncertainties of anthropogenic fluxes leads to an underestimation of the flux signal, and as a result the signal-to-noise ratio.

The high variability in total column XCO₂ signal-to-noise ratio is evident at three TCCON sites (Fig. 15). Over anthropogenic hotspots, shown in table 4, the signal from uncertainty in anthropogenic flux is often found to be comparable to the transport uncertainty (0.1-1.4 ppm).

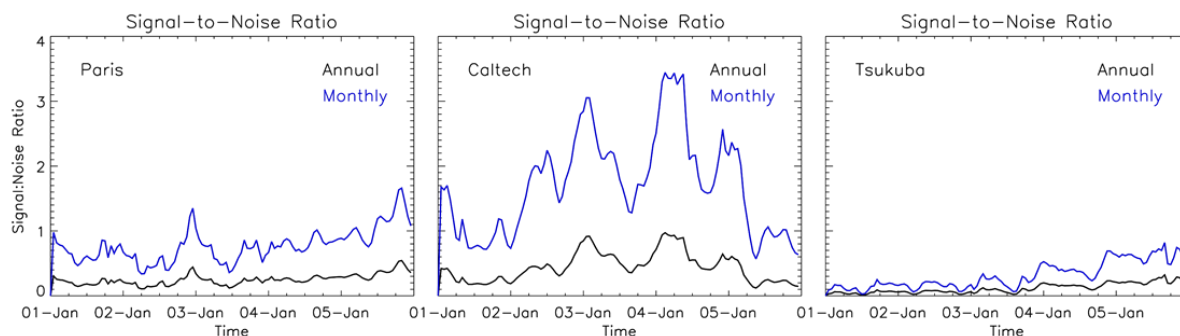


Figure 15 50-member ENS XCO₂ (ppm) signal generated by using annual (black) and monthly (blue) uncertainties in anthropogenic emissions divided by the noise from remaining model error over three TCCON sites. (Adapted from McNorton et al., submitted).

Table 4. Average, minimum and maximum total column model CO₂ error statistics for the transport model error and the atmospheric response to monthly emission uncertainties (signal), and the signal-to-noise ratio for various emission hotspots for January 2015. Results are calculated from the 50-member IFS ensemble. * Denotes large power stations. (Adapted from McNorton et al., submitted).

Location	Transport Error (ppm)	Transport Error (min-max, ppm)	Emission Signal (ppm)	Emission Signal (min-max, ppm)	Signal-to-Noise Ratio
Johannesburg	0.24±0.08	0.10-0.62	0.19±0.07	0.10-0.40	0.79±0.34
London	0.12±0.03	0.05-0.22	0.05±0.02	0.02-0.15	0.39±0.17
Los Angeles	0.55±0.43	0.06-2.23	0.91±0.43	0.26-1.97	1.66±1.16
Moscow	0.19±0.11	0.05-0.71	0.23±0.09	0.12-0.65	1.23±0.76
New York	0.15±0.08	0.05-0.48	0.19±0.09	0.06-0.47	1.29±0.72
Riyadh	0.14±0.10	0.06-0.81	0.28±0.13	0.11-0.75	2.07±0.77
Seoul	0.19±0.13	0.05-0.86	0.21±0.15	0.03-0.79	1.09±0.49
Shanghai	0.65±0.57	0.15-3.75	1.44±0.63	0.60-4.29	2.20±0.97
Singapore	0.22±0.07	0.12-0.56	0.09±0.03	0.04-0.18	0.39±0.14
Tokyo	0.79±0.95	0.09-5.50	0.28±0.27	0.04-1.38	0.36±0.24
Kendal* (RSA)	0.33±0.15	0.08-0.88	0.15±0.05	0.07-0.29	0.44±0.20
Waigaoqiao* (CHN)	0.42±0.28	0.14-1.27	0.74±0.63	0.15-2.57	1.77±0.81
Neurath* (DEU)	0.14±0.07	0.06-0.59	0.06±0.03	0.02-0.18	0.41±0.22

6 Potential applications

The CHE 9km global nature run captures the main source of CO₂ variability associated with biogenic fluxes, emissions and atmospheric transport. CO₂, CH₄, CO and their tagged tracers are available together with the meteorological data.

Potential applications include:

- Observing System Simulation Experiments and Quantitative Network Design experiments to assess the impact of current CO₂ observing system (e.g. Crisp et al, 2018).

- Boundary conditions for regional simulations (e.g. CHE D2.1).
- Comparison/collocation of different observations (e.g. Guerlet et al., 2013).
- Estimation of representation error (e.g. Agusti-Panareda et al., 2019, Kaminski et al., 2019).
- Estimation of transport error (from ensemble simulation, e.g. McNorton et al., 2019).
- Estimation of Jacobians (from ensemble simulations, e.g. McNorton et al., 2019).

7 Conclusion

This report documents the production of the second (Tier 2) global nature run of the CHE project. The main scope of the Tier 2 nature run is to provide boundary conditions to the higher resolution regional models in WP2, as part of an effort to create a library of simulations that can be used in OSSEs to support the design of new CO₂ observing systems. Because time was of essence, this nature run has used the CAMS high resolution CO₂ forecast configuration, which did not require any previous testing. The results shown in this report illustrate the realism of the CO₂ variability at different scales and document the biases and standard errors at several surface and TCCON sites. The errors from the Tier 1 global nature run, which were associated with the prescribed fluxes (e.g. anthropogenic emissions and ocean fluxes) are reduced using upgraded anthropogenic emissions and biogenic representation and the new CAMS GHG re-analysis as initial conditions. Also included is an ensemble of simulations at lower resolution, which provides information on the atmospheric response to uncertainty in the anthropogenic emissions from WP3 and the uncertainty of the transport based on the Ensemble Data Assimilation system at ECMWF.

8 Acknowledgements

The evaluation of the nature run has been performed with observations from Environment Canada (Doug Worthy), National Oceanic and Atmospheric Administration ([Arlyn Andrews](#)) and the TCCON data at Sodankylä (Kivi, Heikkinen and Kyrö from the Finnish Meteorological Institute, Finland), at Garmisch (Ralf Sussmann, KIT, Germany), at Tsukuba (Isamu Morino, NIES, Japan) and at Darwin (David Griffith, University of Wollongong, Australia). The authors are grateful for the guidance from Greet Janssen-Maenhout (JRC) on anthropogenic emissions, Hugo Denier van der Gon (TNO), Marc Guevara (BSC) for the provision of the CAMS81 daily residential heating profiles, CAMS81 (Nellie Elguindi-Solmon and Claire Granier) for the provision of CAMS81 emissions for CO and CH₄, and Christian Rodenbeck for the provision of the CO₂ ocean fluxes.

9 References

- CHE D2.1: J.-M. Haussaire, D. Brunner, J. Marshall, P. Prunet, A. Agusti-Panareda, A. Manders, A.J. Segers, H. Denier van der Gon (TNO), G. Maenhout (JRC), S. Houweling (SRON), M. Krol (WU): Model systems and simulation configurations, March 2018.
- CHE D2.2: Anna Agusti-Panareda (ECMWF) , The CHE tier1 nature run, June 2018.
- CHE D3.3: Margarita Choulga (ECMWF) and Greet Janssens-Maenhout (JRC), Fossil CO₂ emissions per sector, July 2019.

Agustí-Panareda, A., S. Massart, F. Chevallier, S. Boussetta, G. Balsamo, A. Beljaars, P. Ciais, N.M. Deutscher, R. Engelen, L. Jones, R. Kivi, J.-D. Paris, V.-H. Peuch, V. Sherlock, A. T. Vermeulen, P.O. Wennberg, and D. Wunch: Forecasting global atmospheric CO₂, *Atmos. Chem. Phys.*, 14, 11959–11983, 2014.

Agustí-Panareda, A., S. Massart, F. Chevallier, G. Balsamo, S. Boussetta, E. Dutra, A. Beljaars: A biogenic CO₂ flux adjustment scheme for the mitigation of large-scale biases in global atmospheric CO₂ analyses and forecasts, *Atmos. Chem. Phys.*, 16, 10399–10418, 2016.

Agustí-Panareda, A., M. Diamantakis, V. Bayona, F. Klappenbach, and A. Butz: Improving the inter-hemispheric gradient of total column atmospheric CO₂ and CH₄ in simulations with the ECMWF semi-Lagrangian atmospheric global model, *Geosci. Model Dev.*, 10, 1–18, 2017.

Agustí-Panareda, A., Diamantakis, M., Massart, S., Chevallier, F., Muñoz-Sabater, J., Barré, J., Curcoll, R., Engelen, R., Langerock, B., Law, R. M., Loh, Z., Morguá, J. A., Parrington, M., Peuch, V.-H., Ramonet, M., Roehl, C., Vermeulen, A. T., Warneke, T., and Wunch, D.: Modelling CO₂ weather – why horizontal resolution matters, *Atmos. Chem. Phys.*, 19, 7347–7376, <https://doi.org/10.5194/acp-19-7347-2019>, 2019.

Agustí-Panareda, A., J. McNorton, et al., The CHE global CO₂, CH₄ and CO nature runs, ESSD, in preparation, 2019.

Balzarolo, M., Boussetta, S., Balsamo, G., Beljaars, A., Maignan, F., Calvet, J.-C., Lafont, S., Barbu, A., Poulter, B., Chevallier, F., Szczypta, C., and Papale, D.: Evaluating the potential of large-scale simulations to predict carbon fluxes of terrestrial ecosystems over a European Eddy Covariance network, *Biogeosciences*, 11, 2661–2678, doi:10.5194/bg-11-2661-2014, 2014.

Bechtold, P., Köhler, M., Jung, T., Doblas-Reyes, F., Leutbecher, M., Rodwell, M., Vitart, F., and Balsamo, G.: Advances in simulating atmospheric variability with the ECMWF model: From synoptic to decadal time-scales, *Q. J. Roy. Meteor. Soc.*, 134, 1337–1351, 2008.

Bechtold, P., Semane, N., Lopez, P., Chaboureau, J.-P., Beljaars, A., and Bormann: Representing equilibrium and nonequilibrium convection in large-scale models, *J. Atmos. Sci.*, 71, 734–753, 2014.

Beljaars, A. and Viterbo, P.: The role of the boundary layer in a numerical weather prediction model, in: *Clear and cloudy boundary layers*, Royal Netherlands Academy of Arts and Sciences, North Holland Publishers, Amsterdam, 1998.

Bergamaschi, P., Frankenberg, C., Meirink, J. F., Krol, M., Villani, M. G., Houweling, S., Dentener, F., Dlugokencky, E. J., Miller, J. B., Gatti, L. V., Engel, A., and Levin: Inverse modeling of global and regional CH₄ emissions using SCIAMACHY satellite retrievals, *J. Geophys. Res.*, 114, D22301, doi: 10.1029/2009JD012287, 2009.

Boussetta, S., Balsamo, G., Beljaars, A., Agustí-Panareda, A., Calvet, J.-C., Jacobs, C., van den Hurk, B., Viterbo, P., Lafont, S., Dutra, E., Jarlan, L., Balzarolo, M., Papale, D., and van der Werf, G.: Natural carbon dioxide exchanges in the ECMWF Integrated Forecasting System: implementation and offline validation, *J. Geophys. Res.-Atmos.*, 118, 1–24, doi:10.1002/jgrd.50488, 2013.

Buizza, R., Milleer, M. and Palmer, T.N.: Stochastic representation of model uncertainties in the ECMWF ensemble prediction system. *Q. J. Roy. Meteor. Soc.*, 125(560), 2887-2908, 1999.

Buizza, R., M. Alonso Balmaseda, A. Brown, S. English, R. Forbes, A. Geer, T. Haiden, M. Leutbecher, L. Magnusson, M. Rodwell, M. Sleigh, T. Stockdale, F. Vitart, N. Wedi, The development and evaluation process followed at ECMWF to upgrade the Integrated Forecasting System (IFS), ECMWF Technical Memorandum, No. 829, October 2018.

Chevallier, F. P. Ciais, T.J. Conway, T. Aalto, b.E. Anderson, P. Bousquet, E.G. Brunke, L. Ciattaglia, Y. Esaki, M. Frohlich, A. Gomez, A.J. Gomez-Peaez, L. Haszpra, P.B. Krummel, R. L. Langenfelds, M. Leuenberger, T. Machida, F. Maignan, H. Matsueda, J.A. Morgui, H. Mukai, T. Nakazawa, P. Peylin, M. Ramonet, L. Rivier, Y. Sawa, M. Schmidt, L.P. Steele, S.A. Vay, A.T. Vermeulen, S. Wofsy, D. Worthy: CO₂ surface fluxes at grid point scale estimated from a global 21 year reanalysis of atmospheric measurements, *J. Geophys. Res.*, 115, D21307, doi:10.1029/2010JD013887, 2010.

Ciais, P., Crisp, D., Gon, H. v. d., Engelen, R., Heimann, M., Janssens-Maenhout, G., Rayner, P., and Scholze, M.: Towards a European Operational Observing System to Monitor Fossil CO₂ emissions - Final Report from the expert group. European Commission, Copernicus Climate Change Service, http://www.copernicus.eu/sites/default/files/library/CO2_Report_22Oct2015.pdf, 2015.

Claeyman, M. J.-L. Attie, L. El Amraoui, D. Cariolle, V.-H. Peuch, H. Teysse, B. Josse, P. Ricaud, S. Massart, A. Piacentini, J.-P. Cammas, N. J. Livesey, H. C. Pumphrey, and D. P. Edwards : A linear CO chemistry parameterization in a chemistry-transport model: evaluation and application to data assimilation, *Atmos. Chem. Phys.*, 10, 6097–6115, 2010.

Crisp et al. (2018): A constellation architecture for monitoring CO₂ and CH₄ from space, CEOS Atmospheric Composition Virtual Constellation Greenhouse Gas Team.

Diamantakis, M. and A. Agustí-Panareda: A positive definite tracer mass fixer for high resolution weather and atmospheric composition forecasts, ECMWF Technical Memorandum No. 819, <https://www.ecmwf.int/sites/default/files/elibrary/2017/17914-positive-definite-tracer-mass-fixer-high-resolution-weather-and-atmospheric-composition.pdf>, December 2017.

Granier, C., Bessagnet, B., Bond, T., D'Angiola, A., Denier van der Gon, H., Frost, G. J., Heil, A., Kaiser, J. W., Kinne, S., Klimont, Z., Kloster, S., Lamarque, J.-F., Liousse, C., Masui, T., Meleux, F., Mieville, A., Ohara, R., Raut, J.-C., Riahi, K., Schultz, M. G., Smith, S. G., Thompson, A., van Aardenne, J., van der Werf, G. R., and van Vuuren, D. P.: Evolution of anthropogenic and biomass burning emissions of air pollutants at global and regional scales during the 1980–2010 period, *Clim. Change*, 109, 163–190, doi:10.1007/s10584-011-0154-1, 2011.

Griffith, D. W. T., N. Deutscher, V. A. Velazco, P. O. Wennberg, Y. Yavin, G. Keppel Aleks, R. Washenfelder, G. C. Toon, J.-F. Blavier, C. Murphy, N. Jones, G. Kettlewell, B. Connor, R. Macatangay, C. Roehl, M. Ryzek, J. Glowacki, T. Culgan, G. Bryant: TCCON data from Darwin, Australia, Release GGG2014R0. TCCON data archive, hosted by CaltechDATA, California Institute of Technology, Pasadena, CA, U.S.A. <http://doi.org/10.14291/tcon.ggg2014.darwin01.R0/1149290>, 2017.

Guerlet, S., Butz, A., Schepers, D., Basu, S., Hasekamp, O.P., Kuze, A., Yokota, T., Blavier, J.-F., Deutscher, N. M., Griffith, D. W. T., Hase, F., Kyro, E., Morino, I., Sherlock, V., Sussmann, R., Galli, A., and Aben, I.: Impact of aerosol and thin cirrus on retrieving and validating XCO₂ from GOSAT shortwave infrared measurements, *J. Geophys. Res.-Atmos.*, 118, 4887–4905, <https://doi.org/10.1002/jgrd.50332>, 2013.

Haiden, T, Janousek, M, Bidlot, J-R, Ferranti, L, Prates, F, Vitart, F, Bauer, P, Richardson, D (2017). Evaluation of ECMWF forecasts, including 2016-2017 upgrades, ECMWF Technical Memorandum, No. 817, ECMWF, <https://www.ecmwf.int/en/elibrary/17913-evaluation-ecmwf-forecasts-including-2016-2017-upgrades>

Hortal, M.: The development and testing of a new two-time level semi-Lagrangian scheme (SETTLES) in the ECMWF forecast model, *Q. J. Roy. Meteor. Soc.*, 128, 1671–1687, doi:10.1002/qj.200212858314, 2002.

Inness, A., Blechschmidt, A.-M., Bouarar, I., Chabrillat, S., Crepulja, M., Engelen, R. J., Eskes, H., Flemming, J., Gaudel, A., Hendrick, F., Huijnen, V., Jones, L., Kapsomenakis, J.,

Katragkou, E., Keppens, A., Langerock, B., de Mazière, M., Melas, D., Parrington, M., Peuch, V. H., Razinger, M., Richter, A., Schultz, M. G., Suttie, M., Thouret, V., Vrekoussis, M., Wagner, A., and Zerefos, C.: Data assimilation of satellite-retrieved ozone, carbon monoxide and nitrogen dioxide with ECMWF's Composition-IFS, *Atmos. Chem. Phys.*, 15, 5275-5303, doi:10.5194/acp-15-5275-2015, 2015.

Inness, A., Ades, M., Agustí-Panareda, A., Barré, J., Benedictow, A., Blechschmidt, A.-M., Dominguez, J. J., Engelen, R., Eskes, H., Flemming, J., Huijnen, V., Jones, L., Kipling, Z., Massart, S., Parrington, M., Peuch, V.-H., Razinger, M., Remy, S., Schulz, M., and Suttie, M.: The CAMS reanalysis of atmospheric composition, *Atmos. Chem. Phys.*, 19, 3515–3556, <https://doi.org/10.5194/acp-19-3515-2019>, 2019.

IPCC 2006: IPCC Guidelines for National Greenhouse Gas Inventories, Prepared by the National Greenhouse Gas Inventories Programme, Eggleston H.S., Buendia L., Miwa K., Ngara T. and Tanabe K. (eds). Published: IGES, Japan, 2006.

Isaksen, L., Bonavita, M., Buizza, R., Fisher, M., Haseler, J., Leutbecher, M. and Raynaud, L.: Ensemble of data assimilations at ECMWF. Research Department Technical Memorandum No. 636, ECMWF, Shinfield Park, Reading RG29AX, UK, (available online at: <http://www.ecmwf.int/publications/>), 2010.

Janssens-Maenhout, G., Crippa, M., Guizzardi, D., Muntean, M., Schaaf, E., Dentener, F., Bergamaschi, P., Pagliari, V., Olivier, J. G. J., Peters, J. A. H. W., van Aardenne, J. A., Monni, S., Doering, U., Petrescu, A. M. R., Solazzo, E., and Oreggioni, G. D.: EDGAR v4.3.2 Global Atlas of the three major greenhouse gas emissions for the period 1970–2012, *Earth Syst. Sci. Data*, 11, 959–1002, <https://doi.org/10.5194/essd-11-959-2019>, 2019.

Kaiser, J. W., Heil, A., Andreae, M. O., Benedetti, A., Chubarova, N., Jones, L., Morcrette, J.-J., Razinger, M., Schultz, M. G., Suttie, M., and van der Werf, G. R.: Biomass burning emissions estimated with a global fire assimilation system based on observed fire radiative power, *Biogeosciences*, 9, 527–554, doi:10.5194/bg-9-527-2012, 2012.

Kaminski et al. (2019): Atmospheric CO₂ observations from space can support national inventories. Under Review with *Nature Communications*

Kivi, R., Heikkinen, P., Kyrö, E. TCCON data from Sodankylä (FI), Release GGG2014.R0, doi: 10.14291/tcon.ggg2014.sodankyla01.R0/1149280, 2017.

Koehler, M., Ahlgrimm, M., and Beljaars, A.: Unified treatment of dry convective and stratocumulus-topped boundary layers in the ecmwf model, *Q. J. Roy. Meteor. Soc.*, 137, 43–57, 2011.

Leutbecher, M. and Palmer, T.N.: Ensemble forecasting. *Journal of Computational Physics*, 227(7), 3515-3539, 2008.

Leutbecher, M., Lock, S.J., Ollinaho, P., Lang, S.T., Balsamo, G., Bechtold, P., Bonavita, M., Christensen, H.M., Diamantakis, M., Dutra, E. and English, S.: Stochastic representations of model uncertainties at ECMWF: state of the art and future vision. *Quarterly Journal of the Royal Meteorological Society*, 143(707), 2315-2339, 2017.

Malardel, S., N. Wedi, W. Deconinck, M. Diamantakis, C. Kühnlein, G. Mozdzynski, M. Hamrud, P. Smolarkiewicz (2016), A new grid for the IFS, *ECMWF Newsletter No. 146*, <https://www.ecmwf.int/sites/default/files/elibrary/2016/17262-new-grid-ifs.pdf>

Masarie, K. A., Peters, W., Jacobson, A. R., and Tans, P. P.: ObsPack: a framework for the preparation, delivery, and attribution of atmospheric greenhouse gas measurements, *Earth Syst. Sci. Data*, 6, 375-384, <https://doi.org/10.5194/essd-6-375-2014>, 2014.

Massart, S., Agustí-Panareda, A., Aben, I., Butz, A., Chevallier, F., Crevoisier, C., Engelen, R., Frankenberg, C., and Hasekamp, O.: Assimilation of atmospheric methane products into

the MACC-II system: from SCIAMACHY to TANSO and IASI, *Atmos. Chem. Phys.*, 14, 6139–6158, doi:10.5194/acp-14-6139-2014, 2014.

Massart, S., Agustí-Panareda, A., Heymann, J., Buchwitz, M., Chevallier, F., Reuter, M., Hilker, M., and Burrows, J.: Ability of the 4D-Var analysis of the GOSAT BESD XCO₂ retrievals to characterize atmospheric CO₂ at large and synoptic scales, *Atmos. Chem. Phys.*, 16, 1653–1671, doi:10.5194/acp-16-1653-2016, 2016.

McNorton, J., Bousserez, N., Agustí-Panareda, A., Balsamo, G., Choulga, M., Dawson, A., Engelen, R., Kipling, Z., Lang, S., (2019) Diagnosing Model Uncertainty of Global Atmospheric CO₂, *Geoscientific Model Development*, submitted.

ObsPack (2107). Multi-laboratory compilation of atmospheric carbon dioxide data for the period 1957–2016; *obspace_co2_1_GLOBALVIEWplus_v3.2_2017-11-02*, NOAA Earth System Research Laboratory, Global Monitoring Division, <http://dx.doi.org/10.15138/G3704H>

Olivier and G. Janssens-Maenhout, CO₂ Emissions from Fuel Combustion -- 2012 Edition, IEA CO₂ report 2012, Part III, Greenhouse-Gas Emissions, ISBN 978-92-64-17475-7.

http://edgar.jrc.ec.europa.eu/news_docs/jrc-2015-trends-in-global-co2-emissions-2015-report-98184.pdf, 2015.

Rödenbeck, C., Bakker, D. C. E., Metzl, N., Olsen, A., Sabine, C., Cassar, N., Reum, F., Keeling, R. F., and Heimann, M.: Interannual sea–air CO₂ flux variability from an observation-driven ocean mixed-layer scheme, *Biogeosciences*, 11, 4599–4613, <https://doi.org/10.5194/bg-11-4599-2014>, 2014.

Sandu, I., Beljaars, A., Bechtold, P., Mauritsen, T., and Balsamo, G.: Why is it so difficult to represent stably stratified conditions in numerical weather prediction (NWP) models?, *J. Adv. Modeling Earth Syst.*, 5, 1–17, doi:10.1002/jame.20013, 2013.

Spanhi, R., R. Wania, L. Need, M. van Weele, I. Pison, P. Bousquet, C. Frankenberg, P.N. Foster, F. Joos, I.C. Prentice and P. van Velthoven: Constraining global methane emissions and uptake by ecosystems, *Biogeosciences*, 8, 1643–1665, 2011.

Sussmann, R. and Rettinger, M. TCCON data from Garmisch (DE), Release GGG2014.R2, DOI: 10.14291/tcon.ggg2014.garmisch01.R2, 2017.

Takahashi, T., Sutherland, S., Wanninkhof, R., Sweeney, C., Feely, R., Chipman, D., Hales, B., Friederich, G., Chavez, F., Watson, A., Bakker, D., Schuster, U., Metzl, N., Yoshikawa-Inoue, H., Ishii, M., Midorikawa, T., Nojiri, Y., Sabine, C., Olafsson, J., Arnarson, T., Tilbrook, B., Johannessen, T., Olsen, A., Bellerby, R., Körtzinger, A., Steinhoff, T., Hoppema, M., de Baar, H., Wong, C., Delille, B., and Bates, N. R.: Climatological mean and decadal changes in surface ocean pCO₂, and net sea-air CO₂ flux over the global oceans, *Deep-Sea Res. Pt. II*, 56, 554–577, 2009.

Te, Y., P. Jeseck, C. Janssen. 2017. TCCON data from Paris, France, Release GGG2014R0. TCCON data archive, hosted by CaltechDATA, California Institute of Technology, Pasadena, CA, U.S.A. <https://doi.org/10.14291/tcon.ggg2014.paris01.R0/1149279>

Temperton, C., Hortal, M., and Simmons, A.: A two-time-level semi-Lagrangian global spectral model, *Q. J. Roy. Meteor. Soc.*, 127, 111–126, 2001.

Tiedtke, M.: A comprehensive mass flux scheme for cumulus parameterization in large-scale models, *Mon. Weather Rev.*, 117, 1779–1800, 1989.

Untch, A. and Hortal, M.: A finite-element scheme for the vertical discretization of the semi-Lagrangian version of the ECMWF forecast model, *Q. J. Roy. Meteor. Soc.*, 130, 1505–1530, doi:10.1256/qj.03.173, 2006.

Wennberg et al. (2017): TCCON data from California Institute of Technology, Pasadena, USA, Release GGG2014R1. TCCON data archive, hosted by CaltechData, Caltech, Pasadena, CA, USA.

Wunch, D., Toon, G. C., Wennberg, P. O., Wofsy, S. C., Stephens, B. B., Fischer, M. L., Uchino, O., Abshire, J. B., Bernath, P., Biraud, S. C., Blavier, J.-F. L., Boone, C., Bowman, K. P., Browell, E. V., Campos, T., Connor, B. J., Daube, B. C., Deutscher, N. M., Diao, M., Elkins, J. W., Gerbig, C., Gottlieb, E., Griffith, D. W. T., Hurst, D. F., Jiménez, R., Keppel-Aleks, G., Kort, E. A., Macatangay, R., Machida, T., Matsueda, H., Moore, F., Morino, I., Park, S., Robinson, J., Roehl, C. M., Sawa, Y., Sherlock, V., Sweeney, C., Tanaka, T., and Zondlo, M. A.: Calibration of the Total Carbon Column Observing Network using aircraft profile data, *Atmos. Meas. Tech.*, 3, 1351-1362, <https://doi.org/10.5194/amt-3-1351-2010>, 2010.

10 Annex: Prescribed emissions

Table 5: List prescribed surface fluxes used in Tier2 global nature run

Surface flux	Horizontal resolution	Temporal resolution	Source	References	Notes	Archived
CO ₂ ocean fluxes	4.0x5.0 deg.	Monthly	Jena-CarboScope global sea-air CO ₂ flux based on the SOCAT data set of pCO ₂ observations http://www.bgc-jena.mpg.de/CarboScope (oc_v1.6)	Rödenbeck et al. (2013)	Prescribed parameter. Mass conserving interpolation to model grid and linear temporal interpolation.	Yes
CO ₂ anthropogenic emissions	0.1x0.1 deg.	Monthly	European Commission, Joint Research Centre (JRC)/Netherlands Environmental Assessment Agency (PBL). Emission Database for Global Atmospheric Research (EDGAR), release EDGARv4.3.2 FT2015, http://edgar.jrc.ec	Janssens-Maenhout et al. (2019), CHE D3.3	Prescribed parameter. Mass conserving interpolation to model grid.	Yes

CO₂ HUMAN EMISSIONS 2019

			.europa.eu			
<i>CO₂, CO and CH₄ biomass burning</i>	0.1x0.1 deg.	Daily	GFAS v1.2	Kaiser et al. (2012)	Prescribed parameter. Mass conserving interpolation.	Yes
<i>Total CH₄ emissions excluding biomass burning</i>	0.1x0.1 deg. for anthropogenic emissions and various resolutions for other data sets.	Monthly	Various sources including EDGARv4.3.2 with monthly temporal profiles from EDGARv4.2FT2010 HYMN-LPJ wetland flux climatology Sanderson (1996) for termites, Ridgwell et al. (1999) for soil sink, ocean fluxes from Lambert and Schmidt (1993) and Houweling et al. (1999) for wild animals	CO ₂ report 2016: Olivier J, Janssens-Maenhout G, Muntean M, Peters J. Trends in global CO ₂ emissions: 2016 Report. European Commission ; 2016. JRC 10342 (November 2016) http://edgar.jrc.ec.europa.eu/news_docs/jrc-2016-trends-in-global-co2-emissions-2016-report-103425.pdf Spanhi et al. (2011) for wetland emissions	Prescribed parameter. Mass conserving interpolation to model grid and combination of different climatologies with EDGAR4.3.2 emissions in 2012 extrapolated by CAMS81.	Yes
<i>CO anthropogenic emissions</i>	0.5x0.5 deg.	Monthly	MACCity	Granier et al.	Prescribed parameter. Mass conserving interpolation to model grid.	No

¹ Note that all prescribed fluxes are kept constant throughout the 1-day forecast

Document History

Version	Author(s)	Date	Changes
0.1	Anna Agusti-Panareda, Joe McNorton (ECMWF)	01/12/2019	Initial Version
0.2	Anna Agusti-Panareda, Joe McNorton (ECMWF)	06/12/2019	Version for internal review
1.0	Anna Agusti-Panareda, Joe McNorton (ECMWF)	19/12/2019	Revised version incorporating feedback from DLR and University of Bremen.

Internal Review History

Internal Reviewers	Date	Comments
Johan Strandgren (DLR)	17/12/2019	Approved with comments
Michael Buchwitz (University of Bremen)	17/12/2019	Approved with comments

Estimated Effort Contribution per Partner

Partner	Effort
ECMWF	2
Total	2

This publication reflects the views only of the author, and the Commission cannot be held responsible for any use which may be made of the information contained therein.